
EFFICIENTLY INTEGRATE LARGE LANGUAGE MODELS WITH VISUAL PERCEPTION: A SURVEY FROM THE TRAINING PARADIGM PERSPECTIVE

Xiaorui Ma
School of Data Science
Lingnan University
Hong Kong
xiaoruima@ln.edu.hk

Haoran Xie *
School of Data Science
Lingnan University
Hong Kong
hrxie@ln.edu.hk

S. Joe Qin
School of Data Science
Lingnan University
Hong Kong
joeqin@ln.edu.hk

ABSTRACT

The integration of vision-language modalities has been a significant focus in multimodal learning, traditionally relying on Vision-Language Pretrained Models. However, with the advent of Large Language Models (LLMs), there has been a notable shift towards incorporating LLMs with vision modalities. Following this, the training paradigms for incorporating vision modalities into LLMs have evolved. Initially, the approach was to integrate the modalities through pretraining the modality integrator, named Single-stage Tuning. It has since branched out into methods focusing on performance enhancement, denoted as Two-stage Tuning, and those prioritizing parameter efficiency, referred to as Direct Adaptation. However, existing surveys primarily address the latest Vision Large Language Models (VLLMs) with Two-stage Tuning, leaving a gap in understanding the evolution of training paradigms and their unique parameter-efficient considerations. This paper categorizes and reviews 34 VLLMs from top conferences, journals, and highly cited Arxiv papers, focusing on parameter efficiency during adaptation from the training paradigm perspective. We first introduce the architecture of LLMs and parameter-efficient learning methods, followed by a discussion on vision encoders and a comprehensive taxonomy of modality integrators. We then review three training paradigms and their efficiency considerations, summarizing benchmarks in the VLLM field. To gain deeper insights into their effectiveness in parameter efficiency, we compare and discuss the experimental results of representative models, among which the experiment of the Direct Adaptation paradigm is replicated. Providing insights into recent developments and practical uses, this survey is a vital guide for researchers and practitioners navigating the efficient integration of vision modalities into LLMs.

Keywords Multimodal · Large Language Model · Vision-Language Model · Parameter-Efficient Learning · Instruction Tuning · Reinforcement Learning

1 Introduction

The study of vision-language modalities has long been a significant topic, with numerous works dedicated to utilizing transformer-based models to perform multimodal learning [1, 2]. In the era of Large Language Models (LLMs), multimodal-to-text generation tasks have experienced a paradigm shift from Vision-Language Pretrained Models (VLPs) [3, 4, 5] to integrating LLMs with vision modalities [6, 7, 8, 9]. This shift is driven by the advantages of LLMs in terms of adaptability and reasoning ability. VLPs require per-task fine-tuning to transfer to downstream tasks, while LLMs have strong zero-shot or few-shot adaptation abilities [6], saving the resources needed for per-task tuning. In addition, although VLPs have visual perception abilities, enabling them to identify and caption objects in an image, they lack reasoning capabilities [10]. In contrast, LLMs can leverage their pretrained knowledge to reason with visual information [11, 12, 13], offering a deeper understanding of images. While LLMs have these advantages,

*Corresponding author

leveraging off-the-shelf LLMs for VLPM is challenging due to their integrated architecture [7], where the vision encoder and text encoder are constituted as a single model. In contrast, adding a vision encoder to an LLM is more straightforward, requiring a Modality Integrator (MI) to connect the two models. The resulting model is named as Vision Large Language Models (VLLMs), and the architecture is shown in Figure 1. As LLMs scale, computational resource demands increase, making parameter efficiency critical in building VLLMs [14, 15]. This survey examines the Parameter-Efficient Adaptation (PEA) techniques for incorporating visual modalities into LLMs from the training paradigm perspective. The training paradigms are categorized into three types: Single-stage Tuning, Two-stage Tuning, and Direct Adaptation. The categorization is driven by the fact that each paradigm has distinct motivations for efficiency, and different methods are employed to achieve it.

VLLMs adopting Single-stage Tuning first appeared in the VLPM era. From the parameter efficiency perspective, pretraining a VLPM requires multiple feedforward processes due to the simultaneous use of various learning objectives [1], resulting in the trainable parameters increasing multiplicatively as the model size increases. By adding LLMs with visual perception through a Single-stage Tuning paradigm, in most cases, only an MI is trained to bridge two modalities in one training process [7, 16, 17, 18, 19, 20]. Compared to LLM’s scale, this is also a parameter-efficient strategy. For example, BLIP-2 [7] utilizes Flan-T5-XXL with 11 billion parameters, while MI accounts for 0.89% of the whole model. For downstream tasks generalization, unlike VLPMs that adopt end-to-end per-task fine-tuning, zero-shot, and few-shot learning are adopted in Single-stage Tuning to leverage the pretrained knowledge in LLMs.

However, Single-stage Tuning cannot fully unlock the generalization potential and instruction-following capabilities of LLMs. For better zero-shot transfer to unseen tasks and user intentions understanding, Two-stage Tuning introduces an additional training phase, instruction tuning, that involves fully training LLMs in the second stage [8]. Due to the large size of LLMs, there are three methods to reduce trainable parameters: not training LLM but only the MI in the second stage [7, 21, 22, 23, 24, 16], training the MI while incorporating reparameterization modules into LLMs [8, 25, 26, 27, 28] such as LoRA [29], and utilizing a smaller LLMs [30, 31, 32].

In contrast to Two-stage Tuning aiming to improve VL performance, Direct Adaptation primarily focuses on consuming the least resources to transfer LLM to the VL domain. It skips the pretraining stage and directly finetunes the MI on downstream tasks mainly through multi-task learning without updating LLMs [33, 34, 35, 36, 37, 38, 39, 40, 41]. The design of MI achieves an excellent balance between parameter efficiency and modality fusion performance.

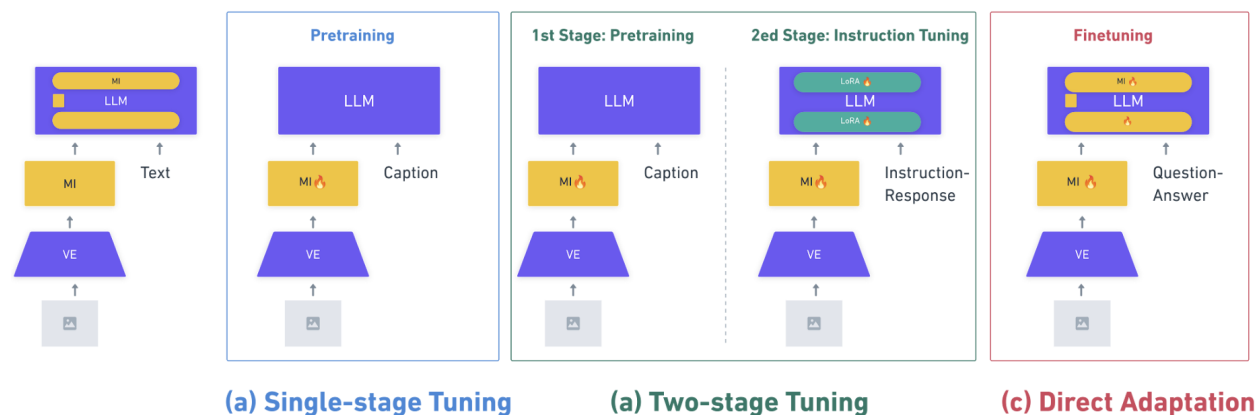


Figure 1: **Integrated Modules and Three Training Paradigms.** MI denotes modality integrator, and VE denotes vision encoder. The trainable module and learning paradigm are the most adopted.

Existing surveys [14, 2], however, mainly focus on the latest VLLMs adopting Two-stage Tuning paradigms. In this survey, the database used is Google Scholar [42], and the keywords are Multimodal, Large Language model, vision-language model, and parameter-efficient learning. The time period is from November 2021 to November 2024. The search results are first screened to match the idea that the model integrates vision modality into LLMs and considers parameter efficiency. Then, more papers are included from the related work of the screened literature. Finally, the quality of the papers is assessed. The inclusion criteria are that the paper needs to be published in the conference ranking A and B in the CCF Recommended List of International Conferences and Periodicals [43], or ICLR. If it does not satisfy the former requirement or it’s an Arxiv paper, the annual citation should exceed 15 times as of November 1st, 2024. Based on this selection process, this review surveys 34 papers on this topic, which are shown in Figure 2. The details of the reviewed models are presented in the Table 1.

In addition, this review is arranged based on the steps to integrate an LLM with visual perception:

1. An LLM is selected as the base model to be augmented with the new modality. (See Section 2) This section introduces the transformer architecture, along with existing PEA methods.
2. A vision encoder is chosen to encode the image into a hidden representation. (See Section 3) This section comprehensively summarizes the architecture and pretrained modalities of employed vision encoders.
3. An MI is designed to transform the visual embedding to the semantic space of LLM. (See Section 4) In this section, the two main categories of modality integrators, Out-of-block Integrators and In-block Integrators, are elaborated.
4. A training paradigm is adopted to transfer LLM to the VL domain. (See Section 5) Three training paradigms, Single-stage Tuning, Two-stage Tuning, and Direct Adaptation, are discussed, with a detailed exploration of the corresponding training techniques, datasets, parameter-efficient strategies, and performance evaluations for each approach.

Finally, we conclude the paper in Section 6.

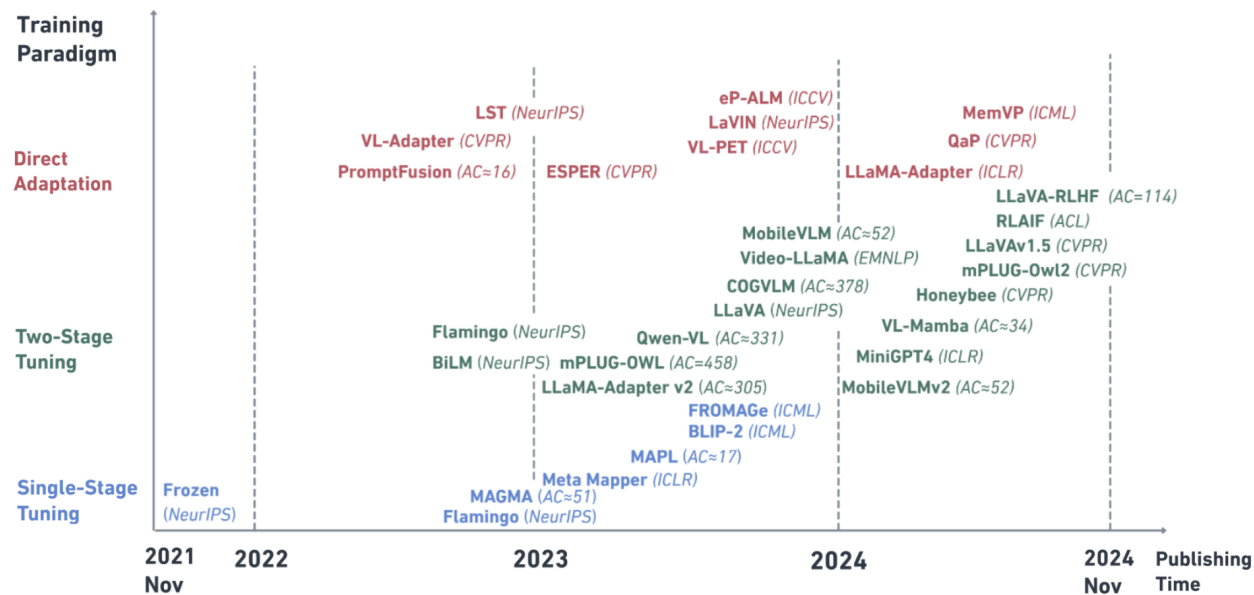


Figure 2: **The Taxonomy and Publishing Time.** AC denotes the annual citation times. For published work, the horizontal axis shows the Published time, while for unpublished work, it shows the submission time to Arxiv.

2 Large Language Model

Large Language Models (MLL) are mainly transformer-based [50] models with encoder [51, 52], encoder-decoder [53, 54] and decoder-only [55, 56, 57, 58, 59, 26, 60] architectures. LLMs utilized in the reviewed paper are summarized in Table 2. In the context of the three training paradigms discussed in this study, the selection of LLMs varies distinctively. Overall, the LLM release time is the key factor for the choice. For the Single-stage Tuning paradigm, the GPT series is typically adopted as this paradigm is early. In the Two-Stage Tuning paradigm, 7B and 13B LLaMA and Vicuna models are generally utilized. Exceptions are that MobileVLM [30, 31], and VLMamba [61] leverage smaller-scale LLMs to enhance efficiency. In the Direct Adaptation paradigm, T5 [53] and Bart [62] are employed as the benchmark LLM due to their manageable sizes [33, 38, 40, 41, 36]. Additionally, there is a notable trend towards adapting LLaMA models in this paradigm [41, 36, 37, 9].

As the preliminaries, the transformer architecture and existing PEA methods for LLMs are introduced in this section.

2.1 Transformer

Transformer [50] comprises an encoder and a decoder, each of which includes L transformer blocks. The basic modules for a transformer block are Multi-Head Attention (MHA) and the Feed-forward Network (FFN). After each module,

Efficiently Integrate Large Language Models with Visual Perception: A Survey from the Training Paradigm Perspective

Model	LLM	LLM Size	Vision Encoder	Modality Integrator	Visual Form	Input	PT	FT	Learning Paradigm	PT size	FT size
Single Stage Tuning											
<u>Frozen</u> [6]	GPT2-like	7B	NF-ResNet-50	Linear Projector	Soft Prompt		MI + VE	-	-	-	-
ClipCap [17]	GPT-2	1.5B	CLIP ViT-B/32	Resampler	Soft Prompt		MI	-	-	3M	-
MAGMA [44]	GPT-J	6B	CLIP-ResNet-50x16	Linear Projector + Bottleneck Adapter [†]	Soft Prompt		MI + VE	-	-	25M	-
<u>Flamingo</u> [16]	Chinchilla	1.4B/7B/70B	NF-ResNet-F6	Resampler + Attention-based Adapter [†]	Prefix		MI	-	-	2.2B	-
MAPL [18]	GPT-J	6B	CLIP ViT-L/14	Resampler	Soft Prompt		MI	-	-	398K	-
ESPER [45]	GPT-2-base	117M	CLIP ViT-B/32	MLP 2x	Soft Prompt		MI	-	RL	-	-
FROMAGe [20]	OPT	6.7B	CLIP ViT-L/14	Linear Projector	Soft Prompt		MI	-	-	3.3M	-
MetaMapper [19]	GPT-2	1.5B	CLIP ViT-B/32	Resampler	Prefix		MI	-	-	330K	-
BLIP-2 [7]	OPT/FlanT5	2.7B/6.7B/3B/11B	ViT-L/14/ ViT-g/14	Q-Former + Linear Projector	Soft Prompt		MI	-	-	129M	-
Two-stage Tuning											
<u>Flamingo</u> [16][3]	Chinchilla	1.4B/7B/70B	NF-ResNet-F6	Resampler + Attention-based Adapter [†]	Prefix		MI	MI	Per-task	2.2B	-
BiLM [23]	DeBERTa	900M	CLIP ViT-L/14	Linear Projector + Bottleneck Adapter [†]	Soft Prompt		MI	MI	Per-task	10M	-
LLaMA-Adapter [37]	LLaMA1	7B	ViT-B/16	Linear Projector + Degree-Adaptive Prefix [‡]	Prefix		MI	Partial MI	Instruction (T+V)	-	-
ESPER [45]	GPT-2-base	117M	CLIP ViT-B/32	MLP 2x	Soft Prompt		MI	MI	RL + Per-task	-	-
LLaVA [8]	LLaMA1	7B	CLIP ViT-L/14	Linear Projector	Soft Prompt		MI	MI + LLM [‡]	Instruction (V)	558K	158K
MiniGPT4 [21]	Vicuna	13B	EVA-CLIP ViT-G	Linear Projector + Q-former	Soft Prompt		Partial MI	Partial MI	Instruction (V)	5M	5K
mPLUG-Owl1 [28]	LLaMA1	7B	CLIP ViT-L/14	Resampler	Soft Prompt		MI + VE	MI + LoRA	Instruction (T+V)	2.1M	102K
LLaMA-Adapter v2 [9]	LLaMA1	7B/65B	CLIP ViT-L/14	Linear Projector + Degree-Adaptive Prefix [‡]	Prefix		MI	Bias, Norm	Instruction (T+V)	567K	52K
Video-LLaMA [24]	LLaMA1/ Vicuna	7B/13B	EVA-CLIP ViT-G/14	Q-Former + Linear Projector	Soft Prompt		MI	MI	Instruction (V)	2M	244K
BLIP-2 [7]	OPT/FlanT5	2.7B/6.7B/3B/11B	ViT-L/14/ ViT-g/14	Q-Former + Linear Projector	Soft Prompt		MI	MI	Per-task	129M	-
QWEN-VL [26]	Qwen	7B	OpenCLIP ViT-bigG-14	Resampler	Soft Prompt		MI + VE	MI + LLM [‡]	Multi-task + Instruction (T+V)	1.4B	50M
LLaVA-RLHF [46]	Vicuna-v1.5	7B/13B	CLIP ViT-L/14	MLP 2x	Soft Prompt		MI+LoRA	MI + LoRA	Instruction (V)+RL	-	-
LLaVA 1.5 [25]	Vicuna-v1.5	7B/13B	CLIP ViT-L/14	MLP 2x	Soft Prompt		MI	MI + LLM [‡]	Instruction (V)	558K	665K
CogVLM-Chat [22]	Vicuna-v1.5	7B	EVA02-CLIP-E/14	MLP2x + Unimodal Linear Adapter [†]	Prefix		MI	MI+VE	Multi-task + Instruction (V)	1.5B	6M
mPLUG-Owl 2 [27]	LLaMA2	7B	CLIP ViT-L/14	Resampler + Unimodal Linear Adapter [†]	Soft Prompt		MI + VE	MI + VE + LLM [‡]	Multi-task + Instruction (T+V)	348M	1.23M
C-Abstractor [47]	Vicuna-v1.5	7B/13B	CLIP ViT-L/14	Convolution-based Abstractor	Soft Prompt		MI	MI + LLM	Multi-task + Instruction (V)	200M	8.13M
D-Abstractor [47]	Vicuna-v1.5	7B/13B	CLIP ViT-L/14	Attention-based Abstractor	Soft Prompt		MI	MI + LLM	Multi-task + Instruction (V)	200M	8.13M
MobileVLM [30]	MobileLLaMA	1.4B/2.7B	CLIP ViT-L/14	Convolution-based Abstractor	Soft Prompt		MI	MI + LLM [‡]	Instruction (V)	558K	665K
MobileVLM v2 [31]	MobileLLaMA	1.4B/2.7B	CLIP ViT-L/14	Convolution-based Abstractor	Soft Prompt		MI + LLM	MI + LLM [‡]	Multi-task + Instruction (V)	1.2M	2.4M
<u>VL-Mamba</u> [32]	Mamba LLM	2.8B	CLIP ViT-L/14	VSS-based Abstractor	Soft Prompt		MI	MI + LLM	Instruction (V)	558K	665K
RLAIF [48]	Vicuna-v1.5	7B/13B	CLIP ViT-L/14	MLP 2x	Soft Prompt		MI + LoRA	MI + QLoRA	Instruction (V) + RL	20K	40k
Direct Adaptation											
VL-Adapter [33]	BART/ T5	139M/220M	CLIP-ResNet-101	Linear Projector + Bottleneck Adapter [†]	Soft Prompt		-	MI	Multi-task	-	-
<u>PromptFusion</u> [35]	GPT3	175B	NF-ResNet-50	-	Soft Prompt		-	Soft Prompt	-	-	-
LST [38]	T5	220M	CLIP-ResNet-101	Linear Projector + Attention-based Adapter [†]	Soft Prompt		-	MI	Multi-task	-	-
eP-ALM [34]	OPT	2.7B	ViT-B/16	Linear Projector	Prefix		-	MI	Per-task	-	-
LaVIN [41]	LLaMA1	7B/13B	CLIP ViT-L/14	MLP2x + Bottleneck Adapter [†]	Soft Prompt		-	MI	Instruction (T+V)	-	-
VL-PET [40]	BART/ T5	139M/220M	CLIP ViT-L/14	Linear Projector + Bottleneck Adapter [†]	Soft Prompt		-	MI	Multi-task	-	-
MemVP [36]	Bart/ LLaMA1	7B/13B	CLIP ResNet-101	Linear Projector	Prefix		-	MI	Per-task	-	-
QaP [39]	DeBERTa	900M	CLIP ViT-L/14	Attention-based Adapter [†] + Bottleneck Adapter [†] + Degree-Adaptive Prefix [‡]	Prefix		-	MI	Per-task	-	-

Table 1: **Summary of Reviewed Models.** MI and VE refer to the Modality Integrator and Vision Encoder. The underlined models are closed-source models, and in open-sourced models, the code of QaP [39] and x-LLM [49] have not yet been released. The PT and FT sizes of BLIP2, Mini-GPT4, mPLUG-Owl, Qwen-VL, and LLaVA v1.5 are from [32]. [†] denotes the In-block Integrators. [‡] denotes that the work provides LoRA-based Tuning in the implementation. Per-task, Multi-task, and Instruction denote Per-task Finetuning, Multi-task Finetuning, and Instruction Tuning. RL denotes reinforcement learning. T and V denote the modality of Instruction Tuning data. The sequence of papers in the table follows the time submitted to Arxiv for consistent comparison with the initial idea.

LLM	Instruction Tuned	Architecture	Release Time	Available Size
GPT-2 [63]	-	Decoder-Only	Feb 2019	117M/345M/774M/1.5B
RoBERTa [51]	-	Encoder-only	Jul 2019	125M/355M
T5 [53]	Flan T5 [62]	Encoder-Decoder	Oct 2019/ Oct 2022	220M/770M/3B/11B
BART [62]	-	Encoder-Decoder	Oct 2019	139M
DeBERTa V2 [52]	-	Encoder-only	Jun 2020	900M/1.5B
GPT-J [64]	-	Decoder-Only	May 2021	6B
Chinchilla [65]	-	Decoder-Only	Mar 2022	70B
OPT [57]	-	Decoder-Only	May 2022	125M/350M/1.3B/2.7B/ 6.7B/13B/30B/66B/175B
LLaMA1 [55]	Vicuna [56]	Decoder-Only	Feb 2023/ Mar 2023	7B/13B/33B/65B
MPT [66]	MPT-Instruct	Decoder-Only	May 2023	1B/7B/30B
RedPajama [67]	RedPajama -Instruct	Decoder-Only	May 2023	3B/7B
LLaMA2 [68]	Vicuna v1.5	Decoder-Only	July 2023/ Aug 2023	7B/13B/34B/70B
Qwen [26]	-	Decoder-Only	Sep 2023	1.8B/7B/14B/72B
MobileLLaMA [30]	-	Decoder-Only	Dec 2023	1.4B/2.7B
Mamba [61]	-	Selective State Space Models	Dec 2023	130M/370M/790M/1.4B/2.8B

Table 2: Summary of LLMs.

there is a Layer Normalization (LN) and a residual connection. For a self-attended MHA, the input embedding X is linearly transformed h times and activated by the attention mechanism to get the head. The concatenated heads will then be projected to the model dimension d .

$$\begin{aligned}
Q &= XW^Q, \quad K = XW^K, \quad V = XW^V, \\
\text{Attention}(Q, K, V) &= \text{softmax} \left(QK^T / \sqrt{D} \right) V, \\
\text{MultiHead}(Q, K, V) &= [\text{head}_1; \dots; \text{head}_h] \cdot W^O, \\
\text{where head}_i &= \text{Attention}(QW_i^Q, KW_i^K, VW_i^V),
\end{aligned} \tag{1}$$

and the parameter size of the linear layers are $W_i^Q \in \mathbb{R}^{d \times d_q}$, $W_i^K \in \mathbb{R}^{d \times d_k}$, $W_i^V \in \mathbb{R}^d \times d_v$, $W^O \in \mathbb{R}^{hd_v \times d}$. The mathematical notations are summarized in the Table 3. In cross-attention, the queries are derived from the target sequence, while the keys and values come from a context sequence, which is different from self-attention, where all values are from the same input. The FFN module is an MLP composed of two linear layers and activated by RELU.

$$\text{FFN}(X) = \sigma(XW_1)W_2, \tag{2}$$

where $\sigma(x) = \max(0, x)$.

Based on the transformer architecture, LLaMA 1 [55] improves LM to RMSNorm, changing ReLU activation into SwiGLU activation [69], further enhancing the model’s nonlinear expression. LLaMA 2 [68] replaces MHA with Grouped-Query Attention, where KV projections are shared across groups of heads instead of all heads.

2.2 Parameter-Efficient Adaptation

PEA is a solution that transfers LLMs to new tasks by updating a small number of parameters [15]. Typically, there are three categories of methods: Prompt-based Tuning [70, 71], Adapter-based Tuning [72], LoRA-based Tuning [29, 73, 74]. In the multimodal context, these ideas are inherited in a way that the visual feature is fed into the LLMs in the form of visual prompts or prefixes, following which the visual modality is fused with textual modality by adapters or LoRA.

2.2.1 Prompt-based Tuning

The prompt-based method is to add trainable embeddings to the LLM input. The prompt-based method can be divided into prefix tuning and soft prompt tuning, which differs in that the soft prompt tuning only adds trainable vectors at the very first input. In contrast, the prefix tuning adds trainable queries to the input for each transformer layer. In the multimodal context, soft prompts and prefixes are the forms of visual embedding input into the LLM.

Prefix Tuning The prefix tuning [70] adds a trainable prefix to the input layer and each transformer layer. As the subsequent generation is conditioned on the prefix, it can serve as a learnable instruction for different downstream tasks.

Notation	Description
Matrix	
I, T	The raw input to the MLLM, i.e. image, text.
X, X_v, X_t	The embedding output by vision encoder or tokenizer.
P', P'_v, P'_t	The random-initialized soft prompt or prefix.
P, P_v, P_t	The output soft prompt or prefix.
S, S_v, S_t	The output of the attention module in the transformer block.
h_i^t	The output of i -th transformer block and t -th timestep.
\hat{Y}	The output of LLM.
Y	The ground truth Label.
Size	
L	The number of transformer blocks in an Attention-based Integrator or LLM.
n, n_v, n_t	The length of embedding.
d, d_v, d_t	The dimension of embedding.
r	The low rank.
Parameter	
ϕ	The frozen parameters, usually refer to the frozen LLMs' parameters.
θ	The trainable parameters.
Network	
$W_i(\cdot)$	The i th linear layer in an MLP.
$W_{down}(\cdot)$	The down projection layer that reduces the dimension of the input.
$W_{up}(\cdot)$	The up projection layer that increases the dimension of the input.
$W^Q(\cdot), W_v^Q(\cdot), W_t^Q(\cdot)$	The linear layer that transforms the input into query vectors.
$W^K(\cdot), W_v^K(\cdot), W_t^K(\cdot)$	The linear layer that transforms the input into key vectors.
$W^V(\cdot), W_v^V(\cdot), W_t^V(\cdot)$	The linear layer that transforms the input into value vectors.
$W^O(\cdot)$	The linear layer that transforms the concatenated heads into outputs.
$W_{FFN}(\cdot)$	The feed-forward module in a transformer block in equation 2.
$VE(\cdot)$	The vision encoder that extracts visual features from the image.
$LLM(\cdot)$	The large language model.
$Block(\cdot)$	A transformer block in the Attention-based Integrator or LLM.
$W_{Conv_i}(\cdot)$	The i -th convolution layer.
$W_{PatchWise}(\cdot)$	The point-wise convolution layer that convolutes with a kernel size of 1.
$W_{DepthWise}(\cdot)$	The depth-wise convolution layer that convolutes independently over each channel.
$W_{BatchNorm}(\cdot)$	The batch normalization layer.
$W_{LayerNorm}(\cdot)$	The layer normalization layer.
$ResBlock_i(\cdot)$	The i -th residual block in equation 8.
$CLIP-T(\cdot)$	The text encoder of CLIP.
Operation	
$[:]$	The concatenation.
$Attention(\cdot)$	The attention mechanism in equation 1.
$Softmax(\cdot)$	The softmax operation.
$\sigma(\cdot)$	The activation function.

Table 3: **The Mathematical Notations.**

For the timesteps within the prefix length p , the transformer layer output is the updated prefix embedding P , and for the later timesteps, which are the textual inputs, the output is from the frozen language model but conditioned on P . Instead of directly updating the prefix embedding P'_θ , an MLP and a smaller matrix (P') are used for parameterization, thus ensuring the training stability. The output of the t -th timestep can be formulated as:

$$h^t = \begin{cases} P[t, :] = \text{MLP}_\theta(P'[t, :]), & \text{if } t \in p, \\ \text{LM}_\phi([P; X], h^{<t}), & \text{otherwise.} \end{cases} \quad (3)$$

$$h^t = [h_1^t; \dots; h_n^t],$$

where $P_\theta \in p \times d$ and h^t are the concatenation of the output of all transformer layers at timestep t .

Soft Prompt Tuning Lester et al. [71] simplifies the prefix tuning idea to add a trainable prompt only to the input of the language model as a learnable instruction to guide the model to perform different downstream tasks. The model is now maximizing $\Pr_{\phi; \theta}(Y | [P; X])$, where θ is the soft prompt parameter and ϕ is the frozen LLM’s parameter, and the shape of the input matrix is that $[P; X] \in \mathbb{R}^{(p+n) \times d}$.

In addition to the textual prompt tuning, Visual Prompt Tuning (VPT) [75] proposes the visual version of prompt tuning (VPT- shallow) and prefix tuning (VPT- deep), which is to add learnable vector in the input layer and in each transformer layer respectively. For both scenarios, the input to the first transformer encoder layer is $[X_{[CLS]}; P; X_v]$, where the soft prompt is added after the $[CLS]$ token. For multimodality context, PromptFuse [35] directly adds a soft prompt at the beginning of concatenated visual embedding X_v and text embedding X_t . The input can be formulated as $[P; X_v; X_t]$. The idea of integrating vision modality into the language model by inputting image-conditioned soft prompt originates from Frozen [6]. To avoid hurting the LM’s generalization ability by a relatively small amount of multimodal training data, the LM is kept frozen, and the vision encoder and a linear layer are trainable to align the two modalities. In this way, Frozen only trains 0.56% of the total model parameters. The difference between soft prompt in LLM and in VLLMs is that the former learns the difference between downstream tasks, while the visual soft prompt represents not the difference, but the image-conditioned information.

2.2.2 Adapter-based Tuning

Adapter-based tuning [72] is to insert a trainable parameter-efficient module into the transformer architecture. In NLP, the architecture of adapters is usually the bottleneck structure [72], while different works propose different inserting positions [76, 77] and training strategies [78]. It projects down and up the output matrices over the d dimension, which can be formulated as:

$$\begin{aligned} X &= (\text{ReLU}(XW_{\text{down}}))W_{\text{up}} + X, \\ W_{\text{down}} &\in \mathbb{R}^{d \times r}, W_{\text{up}} \in \mathbb{R}^{r \times d}, \text{ where } r \ll d. \end{aligned} \quad (4)$$

In a multimodal context, the In-block Modality Integrator inherits the idea of adding efficient trainable modules into LLM, but there are various structures in addition to the bottleneck structure. More details are discussed in Section 4.2.

2.2.3 LoRA-based Tuning

LoRA-based tuning is utilized in VLLMs involving updating the LLMs in the second training stage. LoRA [29] updates the transformer weights by decomposing the changing weights to two low-rank matrices, which can be formulated as:

$$\Delta W = BA, W = W_0 + \Delta W, \quad (5)$$

where $B \in \mathbb{R}^{d \times r}$, $A \in \mathbb{R}^{r \times k}$, $r \ll \min(d, k)$. During training, only parameters in the low-rank matrices B and A are updated, keeping the pre-trained parameters W_0 frozen. A set of parameters in B and A can be stored for each downstream task. QLoRA [73] advances the LoRA approach by incorporating weight quantization for the LoRA adapters, reducing them to lower precision. This enhancement significantly decreases both memory usage and storage needs. Decomposed Rank Adaptation (DoRA) [74] further refines the process of model fine-tuning by decomposing the pretrained weights into two components: magnitude and direction. By leveraging LoRA to fine-tune the directional component efficiently, DoRA maintains parameter efficiency while simultaneously avoiding additional inference latency.

2.3 Learning Paradigm

The learning paradigms in VLLMs are adapted from LLMs, including Multi-task learning (MTL), Instruction Tuning, and Reinforcement learning (RL). This section outlines their use in LLMs and briefly covers their adaptation to multimodal settings. The learning paradigms of each model are summarized in Table 1.

2.3.1 Multi-task Learning

MTL refers to training a model to tackle multiple tasks concurrently during a single training phase [79], which utilizes common knowledge across multiple related tasks for better generalization performance [80]. Its complementary approach is per-task learning. MTL has become a key approach in NLP, demonstrating a wide range of applications such as information extraction, natural language understanding, and text generation [81]. In the context of LLMs, MTL has evolved to require adjustment of task-specific weights [82]. In the multimodal domain, task weights are typically determined by the size of the data for each task [33]. The corresponding loss function can be expressed as:

$$\mathcal{L}(D; \theta) = \frac{1}{|D|} \sum_{(I, T, Y) \in D} l(I, T, Y; \theta), \quad (6)$$

where D is the universal VL dataset composed of N datasets $D_1, D_2 \dots D_N$.

2.3.2 Instruction Tuning

VLLMs are designed to enable effective communication with humans, and instruction tuning equips VLLMs with the ability to understand user intentions and respond to commands [83]. Studies have shown that fine-tuning LLMs with instruction data significantly enhances their zero-shot performance on unseen tasks [83]. The instruction data is built by organizing original structured datasets in different ways connected by natural-language instructions. The instruction data with multimodal information is first proposed by LLaVA [8].

2.3.3 Reinforcement Learning

In the LLM context, RL is a learning paradigm where an LLM learns to generate human-preferred outputs by setting the goal of maximizing rewards obtained from human feedback [84], AI feedback [85], or other reward systems [86]. During learning, Proximal Policy Optimization (PPO) [87] is a widely used RL loss function. It limits drastic policy updates through a clipping mechanism, while maximizing the cumulative reward. The standard PPO objective is defined as:

$$\begin{aligned} L^{\text{PPO}}(\theta) &= \mathbb{E}_t [\min(r_t(\theta)A_t, \text{clip}(r_t(\theta), 1 - \epsilon, 1 + \epsilon)A_t)], \\ r_t(\theta) &= \pi_\theta(a_t|s_t) \cdot [\pi_{\theta_{\text{old}}}(a_t|s_t)]^{-1}, \end{aligned} \quad (7)$$

where $r_t(\theta)$ is the ratio of the new and old policy probabilities, A_t is the advantage function that estimates how much better an action is compared to the expected return, and ϵ is a hyperparameter controlling the clipping range. The clipping function ensures that policy updates remain within a constrained range to prevent excessively large updates that destabilize training.

Reinforcement Learning with Human Feedback (RLHF) has become crucial in aligning LLMs with human preferences and ethical considerations [84]. The RLHF pipeline generally consists of three stages. First, in Supervised Fine-tuning (SFT), the LLM is initially tuned by instructions. Second, in Reward Model Training, a separate reward model is trained using human preference on multiple model outputs, ranking them based on quality. Third, the LLM is fine-tuned using the PPO algorithm, backpropagating the LLM parameter. In this setting, the model needs to optimize responses based on users' overall preferences rather than every detail. Therefore, lower computational costs are consumed because it updates the model by utilizing coarse-grained feedback, such as paragraph-level ranking or overall preferences, avoiding fine-grained backpropagation for each token [88]. This approach has been pivotal in enhancing LLMs like ChatGPT [84]. In the multi-modal domain, models like LLaVA-RLHF [46] and RLAIIF [48] adopt a similar training pipeline. Recently, DeepSeek-R1 [86] has improved efficiency by reducing the number of training examples required in SFT and replacing reward model training through the application of a rule-based reward system. In the multi-modal context, ESPER [45] reduces training costs by leveraging unpaired image data and using CLIP similarity as a reward signal.

3 Vision Encoder

To add the visual modality, a pre-trained vision encoder is utilized to extract visual embedding X_v from the input image I . The extracted X_v will be further transformed to feed into LLM. The vision encoders used in the reviewed literature are summarized in Table 4. Overall, CLIP ViT L/14 [89] is the most commonly utilized vision encoder, and there is no clear preference in terms of vision encoders for the three training paradigms.

3.1 Architecture

There are two architectures: Vision Transformer (ViT) [90] and Residual Network (ResNet) [96], between which ViT is more frequently employed. The core idea of ViT [90] is to treat an image as a sequence of patches and regard them as tokens, similar to words in a sentence. Assuming that an image $I \in \mathbb{R}^{h \times w \times c}$, is inputted into the vision encoder, it will first be divided into N patches, where each patch $I_p \in \mathbb{R}^{a \times a \times c}$ and $N = \frac{hw}{p^2}$. Each patch is flattened into a vector, linearly transformed and added with positional encoding, and then encoded by the transformer encoder, which is described in Sec 2.1.

ResNet [96] is a Convolutional Neural Network (CNN). It is composed of a series of residual blocks, with each block consisting of multiple convolutional layers with skip connections. For a residual block with one convolution layer, the first residual block can be formulated as:

$$X'_v = \text{ResBlock}(I) = \text{ReLU}(W_{\text{BatchNorm}}(I \cdot W_{\text{Conv}}) + I). \quad (8)$$

Vision Encoders	Architecture	Parameter Size
Uni-modal		
ViT-B/16 [90]	ViT	86.2M
ViT-L/14 [90]	ViT	304M
NF-ResNet-50 [91]	ResNet	25.6M
NF-ResNet-F6 [91]	ResNet	438.4M
ViT-g/14 [92]	ViT	1.3B
Multimodal		
CLIP ViT-L/14 [89]	ViT	304M
CLIP ViT-B/32 [89]	ViT	87.8M
CLIP-ResNet-101 [89]	ResNet	56.3M
CLIP-ResNet-50x16 [89]	ResNet	167.3M
OpenCLIP ViT-bigG-14 [93]	ViT	1.9B
EVA-CLIP ViT-G/14 [94]	ViT	1B
EVA02-CLIP-E/14 [94]	ViT	4.4B

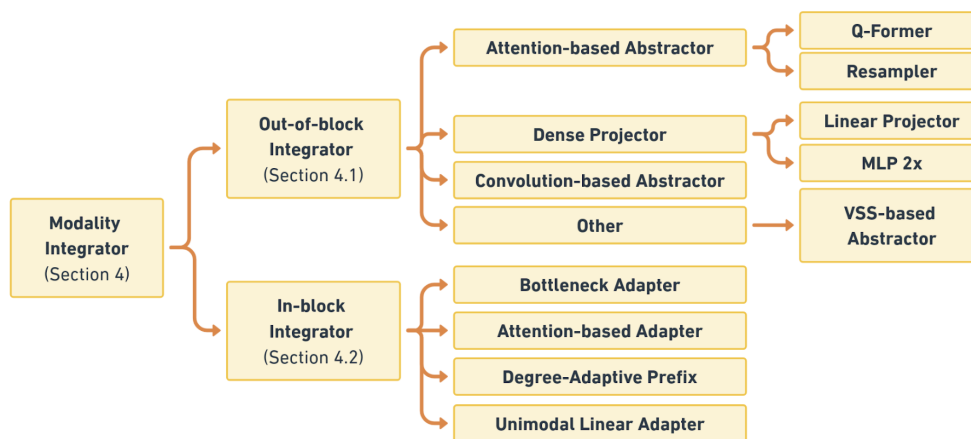
Table 4: **Summary of Vision Encoders.** The models are accessed from the OpenClip repository [95].

3.2 Pretrained Modality

From the modality perspective, both uni-modal and multimodal vision encoders are utilized. Uni-modal vision encoder refers to encoders only pre-trained by images, while multimodal vision encoder is the vision encoder of the CLIP model [89]. CLIP is a VLPM pre-trained with image-text pairs and contrastive loss, which pushes similar text and visual representations closer while pushing the negative samples further. Most VLLMs adopt a multimodal vision encoder. Merullo et al. [97] proves that the more language supervision involved pertaining to the image encoder, the better the performance of language vision tasks. Out of data efficiency considerations, eP-ALM [34] choose a uni-modal vision encoder to avoid using multimodal encoders pretrained on huge datasets.

4 Modality Integrator

The modality integrator is categorized into Out-of-block Integrators and In-block Integrators, where the "block" refers to the LLM. The Out-of-block Integrators, as a basic component of VLLM, align the visual features extracted by vision encoders with the input of LLMs. The In-block Integrators are modules inserted into the LLM architecture, which change the computational graph of LLMs and fuse the multimodal information. The structure of the Modality Integrator is crucial for efficiently integrating the vision modality into the LLM, as it directly impacts the model's ability to process and understand multimodal information and the trainable parameter scale. The taxonomy of MI is shown in Figure 3.

Figure 3: **Taxonomy of Modality Integrator.**

4.1 Out-of-block Integrator

Commonly, the Out-of-block Integrator is the external connector between the vision encoder and LLM, transforming the visual features over length or dimension. Based on the architecture, the Out-of-block Integrator is classified into an Attention-based Abstractor, Dense Projector, Convolution-based Abstractor, and VSS-based Abstractor.

	Attention-based	Linear Mapping	Convolution-based
Maintaining Local Context		✓	✓
Maintaining Global Context	✓		
Adaptability	✓		✓
Parameter efficiency		✓	✓

Table 5: **Comparison of Out-of-block Integrators.** Adaptability refers to the flexibility in adjusting the output token length. The parameter efficiency is compared under the same number of layers.

4.1.1 Attention-based Abstractor

Resampler The Resampler bridges the vision encoder and LLM by inputting visual embedding X_v and fixed-length learnable prompts P'_v into L layers self-attention blocks and outputting the P_v carrying visual information.

In the first transformer block of the Resampler:

$$\begin{aligned}
 h_1 &= \text{Block}_1([X_v; P'_v]), \\
 Q &= P'_v W^Q, K = [X_v; P'_v] W^K, V = [X_v; P'_v] W^V, \\
 h'_1 &= \text{Attention}(Q, K, V) + P'_v, \\
 h_1 &= h'_1 W_\theta^{FFN} + h'_1.
 \end{aligned} \tag{9}$$

In the last transformer layer,

$$P_v = \text{Block}_{L_i}(h_{L_i-1}), \tag{10}$$

where $P'_v \in \mathbb{R}^{p \times d_v}$, $P_v \in \mathbb{R}^{p \times d_t}$.

ClipCap [17] and Flamingo [16] utilize the Resampler as a prefix former, meaning that P_v is fed into each transformer block of the language model. Whereas Meta-Mapper [19] and Qwen-VL [26] regard it as a soft prompt former, P_v is prepended to the textual input for the language generator. In Meta-Mapper, the resampler is self-attended, where the input of Q, K, V are all $[X_v; P_v]$. mPLUG-Owl2 forms the Resampler as a self-attention layer with a SwiGLU activation function [69].

There are two advantages of the Resampler. First, it shortens the length of visual input to the language model and keeps the input length constant, irrespective of the variable length of the original visual embedding [16]. This enables flexibility in the number of images, which is significant in video input. Second, the transformer architecture is more expressive than the linear projection [17], which can capture more representative visual information.

However, Cha et al. [47] argue that self-attention-based Resampler loses visual information because it puts more attention weight on the major object of an image while ignoring insignificant objects. To strengthen the spatial context-capturing capability of the Attention-based Abstractor, Deformable attention [98] is utilized in the D-Abstractor, considering the reference point and learnable offset.

Another drawback is the parameter inefficiency of attention-based structures. To save parameters, MAPL [18] adds down projection layers before the Resampler to reduce the input dimension of the visual embedding X_v and up-project the output P_v to expand its dimension, thus causing a considerable reduction in parameter consumption. The process can be formulated as:

$$\begin{aligned}
 X_{\text{input}} &= [X_v W_{\text{down}}; P_v], & X_{\text{output}} &= P_v W_{\text{up}} \\
 W_{\text{down}} &\in \mathbb{R}^{d_v \times r}, & W_{\text{up}} &\in \mathbb{R}^{r \times d_v}, & \text{where } r < d_v.
 \end{aligned} \tag{11}$$

Q-Former Unlike the Resampler, the Q-former proposed by BLIP-2 [7] involves visual and textual input. Each layer of the Q-former is composed of a self-attention module shared across the learned queries P_{tv} and the input text X_t , a cross-attention layer between image embedding X_v and the soft prompt P_{tv} , and two feed-forward layers for two modalities separately. The feed-forward process is formulated as below.

In the first layer of the Q-former,

$$h_1 = \text{Block}_1([X_v; P'_{tv}; X_t]). \quad (12)$$

For each layer in Q-former, there is a shared self-attention layer between text X_t and learned query P_{tv} , where

$$\begin{aligned} Q &= [P'_{tv}; X_t]W^Q, K = [P'_{tv}; X_t]W^K, V = [P'_{tv}; X_t]W^V \\ h'_{1t} &= \text{Attention}(Q, K, V), \end{aligned} \quad (13)$$

After the shared self-attention module, the two modalities are separated and processed. For the vision stream, the soft prompt is cross-attended with visual embedding X_v and processed by the visual feed-forward layer. The h_{tv} means that the output of this block contains both textual and visual information.

$$\begin{aligned} Q' &= P'_{tv}W^Q, K' = X_vW^K, V' = X_vW^V, \\ h'_{1tv} &= \text{Attention}(h'_{1t}, X_v), \\ h_{1tv} &= h'_{1t}W_\theta^{FFN_v}. \end{aligned} \quad (14)$$

For the text stream, the self-attended h'_{1t} is processed by the textual feed-forward layer.

$$h_{1t} = h'_{1t}W_\theta^{FFN_t}. \quad (15)$$

In the last layer,

$$\begin{aligned} P_{tv} &= \text{Block}_L(h_{L-1tv}), \\ h_t &= \text{Block}_L(h_{L-1t}). \end{aligned} \quad (16)$$

In the first pretraining stage, the Q-former is pre-trained by three tasks to fuse the two modalities: Image text matching, Image contrastive learning, and Image grounded text generation, to align the visual soft prompt to the LLM's encoding space.

In the second pretraining stage, a dense layer is trained to project to the language model input dimension. The parameters are updated by language modelling loss.

$$P_{tv} = \text{Q-Former}(X_v)W_\theta, \quad (17)$$

where $X_v \in \mathbb{R}^{n_v \times d_v}$, $P_{tv} \in \mathbb{R}^{n_p \times d_t}$. BLIP2 pretraining only involves the Q-former and a dense layer, thus saving over 96% of the parameters.

Frozen Q-former is further adopted in Mini-GPT4 [21] and X-LLM [49] to extract text-conditioned visual embedding. X-LLM and Video-Llama [24] also use a trainable Q-Former with a linear layer as the integrator to augment visual and audio perception.

4.1.2 Dense Projector

A Dense Projector is either a single linear layer or a two-layer MLP, which can be formulated as:

$$P_v = X_vW, \quad (18)$$

$$P_v = \sigma(X_vW_1)W_2. \quad (19)$$

It has been proved that a trainable linear projector is capable of translating visual semantic information to an LM-understandable language and can gain comparable performance with end-to-end trained VLMs [97]. FROMAGe [20] uses linear layers to form visual soft prompts for the image captioning tasks and form both textual and visual soft prompts for the ITM tasks. LLaVA [8] uses an MLP to connect frozen LLM and vision encoder. MiniGPT-4 [21] adds a trainable linear layer to connect the frozen vision encoder, Q-former, and LLM, achieving high parameter efficiency.

However, Dense Projector lacks the flexibility to adjust the length of visual representation. To overcome this, the projector output in MemVP [36] is directly fed into the FFN of the LLM transformer block without occupying the input tokens.

In addition to the standalone use of Dense Projectors, its combination with In-block Integrators is frequently employed to achieve deeper modality interaction [33, 22, 37, 44, 23, 40].

4.1.3 Convolution-based Abstractor

Cha et al. [47] spots the limitation of the current Dense Projectors and Attention-based Abstractors. The linear mapper is good at retaining complete visual context while having no flexibility in controlling the output number of visual tokens, which affects the inference efficiency of the MLLM. The attention-based integrator can control the visual token number, while the attention mechanism extracts only the representative subject in the image, leading to visual information loss. To retain both properties, it proposes a C-Abstractor, the architecture of which includes two modules H and Q , which are both composed of N ResNet blocks [99]. They are also connected by an adaptive average pooling layer. The architecture can be formulated as:

$$\begin{aligned} H_1 &= \text{ResBlock}_1(X_v) = \text{ReLU}(W_{\text{BatchNorm}}(X_v \cdot W_{\text{Conv}})), \\ H_N &= \text{ResBlock}_L(H_{N-1}), \\ P &= \text{AdaptiveAvgPool}(H_N), \\ Q_1 &= \text{ResBlock}_{N+1}(P) = \text{ReLU}(W_{\text{BatchNorm}}(P \cdot W_{\text{Conv}})), \\ Q_N &= \text{ResBlock}_{2N}(Q_{N-1}). \end{aligned} \quad (20)$$

MobileVLM series [30, 31] efficiently project the visual embedding X_v through depthwise-convolution $W_{\text{DepthWise}}$ and average pooling $\text{AvgPool}_{2 \times 2}$. For the MobileVLM v1, the Out-of-block Integrator can be formulated as:

$$\mathbf{P}_v = \begin{cases} P''_v &= W_{\text{PatchWise}}(\text{GELU}(W_{\text{PatchWise}}(X_v))), \\ P'_v &= W_{\text{LayerNorm}}[W_{\text{DepthWise}}(W_{\text{LayerNorm}}(W_{\text{DepthWise}}(P''_v)))] + P''_v, \\ P_v &= W_{\text{LayerNorm}}[W_{\text{DepthWise}}(W_{\text{LayerNorm}}(W_{\text{DepthWise}}(P'_v)))] \end{cases} \quad (21)$$

where GELU refers to the non-linear activation function, the input and output sizes are $X_v \in \mathbb{R}^{n_v \times d_v}$, $P_v \in \mathbb{R}^{(n_v/4) \times d_t}$.

MobileVLM v2 adds a Positional Encoding Generator [100] and a residual connection, enabling the architecture to replace one Depth Convolutional layer to average pooling, which reduces over 99% parameters compared to the v1 projector.

$$\mathbf{P}_v = \begin{cases} P''_v &= W_{\text{PatchWise}}(\text{GELU}(W_{\text{PatchWise}}(X_v))), \\ P'_v &= \text{AvgPool}_{2 \times 2}(P''_v), \\ P_v &= W_{\text{DepthWise}}(P'_v) + P'_v. \end{cases} \quad (22)$$

The input and output sizes are $X_v \in \mathbb{R}^{n_v \times d_v}$, $P_v \in \mathbb{R}^{n_v/k^2 \times d_t}$, where k stands for the average kernel size.

4.1.4 Other

VL-Mamba [32] proposes a Vision Selective Scan (VSS) mechanism to capture richer information from the non-causal visual data without increasing parameters. It concatenates the feedforward, backward, horizontal, and vertical scan of image patches and uses an MLP layer or linear layer to process them.

4.2 In-block Integrator

The In-block Integrator here refers to tunable modules inserted into transformer blocks of LLMs. By changing the computational graph of the LLM, the In-block Integrator further fuses the two modalities or controls the degree of the introduced visual information. Commonly, In-block Integrators are adopted together with the external connector. Based on the architecture, the In-block Integrator is classified into Degree-Adaptive Prefix, Bottleneck Adapter, Attention-based Adapter, and Unimodal Linear Adapter.

4.2.1 Bottleneck Adapter

As described in 2.2.2, the Bottleneck Adapter [72] is a typical structure for parameter efficiency. Sung et al. [33] find that in the multimodal context, the adapter carries the information of the introduced modality instead of task-specific knowledge.

MAGMA [44] first attempts to utilize both a Dense Projector and a Bottleneck Adapter. VL-PET [40] proposes four adapter architectures of three parameter sizes. In addition to typical bottleneck architecture, it also adopts a down-projection layer $W'_{\text{down}} \in \mathbb{R}^{d \times 1}$ and copies projected embeddings across the dimension N times to expand to $W_{\text{down}} \in \mathbb{R}^{N \times d}$. In this way, only the parameter W'_{down} is tunable. To deal with mixed modality input, LaVIN [41] proposes a modality classifier to shift between single-modal and multimodal processing adapters automatically. To reduce the parameter, the two adapters share down-sampling projector weights during finetuning.

4.2.2 Attention-based Adapter

The base structure of the Attention-based Adapter is the transformer block as described in 2.1. In Flamingo [16], a fusion adapter called Gated XAtten-Dense is inserted before each LLM transformer block, fusing the visual soft prompt formed by Resampler and the text embedding. The adapter cross-attends two modalities by retrieving text-conditioned visual information. It is composed of a cross-attention sublayer and a feed-forward layer, with TANH gating after each sublayer. For the first adapter layer, the process can be formulated as:

$$\begin{aligned} Q &= X_t W^Q, \quad K = P_v W^K, \quad V = P_v W^V, \\ h'_i &= \text{TANH}(\text{Attention}(Q, K, V)) + X_t, \\ h_i &= \text{TANH}(h'_i W_{\text{FFN}}) + h'_i, \end{aligned} \quad (23)$$

where $\text{TANH}(x) = (e^x - e^{-x}) / (e^x + e^{-x})$.

QaP [39] inserts Resampler (Section 4.1.1) inside the LLM, between the frozen self-attention module and FFN, processing the constant modality query P' . Unlike the common practice, QaP doesn't involve an Out-of-block Integrator but utilizes a standalone internal Resampler to process prefix. It achieves higher parameter efficiency by setting the learnable prefix length as one for each modality.

Considering parameter efficiency and memory efficiency, LST [38] tunes a side network composed of the down-scaled LLM blocks. The weights of each transformer block are shortened proportionally at the dimension level. In this way, not only are the tuned parameters reduced, but the weights are back-propagated through the side network, thus saving the memory for LLMs.

4.2.3 Degree-Adaptive Prefix

Unlike other VLLMs where the prefix is transformed from visual embeddings by Out-of-block Integrators, Degree-Adaptive Prefix is internally informed by LLMs, with their degree controlled by a gating factor [37, 9, 39]. In QaP, the prefix for added modality output by i -th Resampler can be formulated as:

$$\begin{aligned} Q &= P' W^V, \quad K = X_v W^K, \quad V = X_v W^V, \\ P_i &= g_i (\text{Resampler}(Q, K, V)) + X_v, \end{aligned} \quad (24)$$

where g_i represents a tunable gating parameter controlling the degree of modality information.

Considering the disturbance a randomly initialized prefix may cause to the LLM, LLaMA-Adapter [37] proposes a gating parameter to control the weight of the learnable prefix contributing to the next token prediction. Prefix is added to each of the top- l transformer layers, and its disturbance can be minimized by the zero-initialized gating factor at the early training stage. To compute the effect of the prefix token, at each transformer layer, the hidden states of the predictive word are generated, and the effect is quantified by the attention score before softmax. The visual soft prompt is formed by a trainable linear projection and element-wisely added to the prefix at each transformer layer. Suppose the current timestep is k , the attention score of l -th transformer layer can be formulated as:

$$\begin{aligned} Q_l &= X_k^l W_\phi^Q, \quad K_l = [P_v^l, X_{<k}^l; X_k^l] W_\phi^K, \quad V_l = [P_v^l; X_{<k}^l; X_k^l] W_\phi^V, \\ S_l(P_v^l, X_{<k}^l, X_k^l, W_\phi) &= Q K^T / \sqrt{D} \in \mathbb{R}^{1 \times (m+n+1)}, \\ S_l &= [S_l^m; S_l^{n+1}]^T, \\ S_l^q &= [\text{softmax}(S_l^m) \cdot g_l; \text{softmax}(S_l^{n+1})]^T. \end{aligned} \quad (25)$$

The trainable parameters are the prefix P_v , gating parameters g , and the linear projection W_θ .

4.2.4 Unimodal Linear Adapter

Unimodal Linear Adapters are defined as the additional sets of linear layers used to form query, key, and value for the added modality. Compared to mapping the visual features into discrete textual representation space, this method avoids ignoring the rich semantic information in the visual [27]. COGVLM [22] adds a set of query, key, and value projection Layers and a trainable FFN block to process the visual modality. The process can be formulated as:

$$\begin{aligned} Q &= [P_v W_v^Q; X_t W_t^Q], \quad K = [P_v W_v^K; X_t W_t^K], \quad V = [P_v W_v^V; X_t W_t^V], \\ \text{FFN}(S_v, S_t) &= [\text{FFN}_v(S_v); \text{FFN}_t(S_t)]. \end{aligned} \quad (26)$$

mPLUG-Owl 2[27] adopts a similar idea in its Modality-Adaptive Module, and the difference is that no W_v^Q is added.

5 Training Paradigms, Datasets, and Experiment

In this section, we first introduce evaluation benchmarks applicable across all three training paradigms, providing a consistent framework for comparison. Next, we delve into the three primary training paradigms: Single-stage Tuning, Two-stage Tuning, and Direct Adaptation, as illustrated in Figure 1. For each paradigm, we discuss the corresponding training techniques, datasets, parameter-efficient strategies, and performance discussion. Notably, the experiments for VLLMs following the Direct Adaptation paradigm are replicated, and those for other paradigms are sourced from their respective publications or GitHub repositories.

Dataset	Task	Format		Size		Evaluation Matrix	Capability			Basic Info	
		Input	Label	Image #	Question #		Perception	Reasoning	OCR	Source	Time
Traditional											
<u>VQAv2</u> [101]	VQA (short)	$[I, Q]$	Phrases	82783/ 40504/ 81434	443757/ 214354/ 447793	acc.	Basic	-		COCO	2017
OKVQA [102]	VQA (short)	$[I, Q]$	Phrases	-	9009/5046	acc.	Advanced	Advanced		COCO	2019
GQA [103]	VQA (short)	$[I, Q]$	Phrases	113018	22000000	acc.	Basic	Basic		Visual Genome	2019
VisWiz [104]	VQA (short)	$[I, Q]$	Phrases	20523/ 4319/ 8000	20523/ 4319/ 8000	acc.	Advanced	Basic	✓	Photo taken by blind people	2023
TextVQA [105]	TextVQA (short)	$[I, Q]$	Phrases	28408	45336	acc.	Basic	-	✓	Open Images v3 [106]	2024
OCRVQA [107]	TextVQA (short)	$[I, Q]$	Phrases	207572	800000/ 100000/ 100000	acc.	Basic	Basic	✓	[108]	2024
ScienceQA [11]	VQA(MC)	$[I, Q, C, M]$	MC	-	21208	acc.	Basic	Advanced		Scientific problems	2022
COCO Cap- tions [109]	ImageCap	$[I]$	Free-Form Captions	82783/ 40504/ 40775	413915/ 202520/ 379249	CIDEr [110]/ BLEU@4 [111]	Basic	-		COCO	2015
Nocaps [112]	ImageCap	$[I]$	Free-Form Captions	/ 4500/ 10600	166100	CIDEr, SPICE [113]	Basic	-		COCO, Open Images	2019
Flickr30K [114]	ImageCap	$[I]$	Free-Form Captions	29783/ 1000/ 1000	148915/ 5000/ 5000	CIDEr/ BLEU@4	Basic	-			2015
NLVR [115]	NLVR	$[I_1, I_2, Cap]$	Binary		74460/ 5940/ 11844	acc.	Basic	Basic		Google Images	2019
Advanced											
MMBench [12]	VQA(MC)	$[I, Q, M]$	MC	-	3217	CircularEval Top-1 acc.	Advanced	Advanced	✓	Various sources	2024
SEED-1 [116]	VQA(MC)	$[I, Q, M]$	MC [†]	-	15973	acc.	Basic	Advanced	✓	CC3M	2023
LLaVA-Bench [8]	VQA (open)	$[I, Q]$	Free-Form Response [†]	30	90	GPT-4 score	Advanced	Advanced		COCO	2023
LLaVA-Bench (In-the-Wild) [8]	VQA (open)	$[I, Q]$	Free-Form Response [†]	24	60	GPT-4 score	Advanced	Advanced		-	2023
OwlEval [28]	VQA (open)	$[I, Q]$	Free-Form Response	50	82	Manual evaluation [117]	Advanced	Advanced	✓	MiniGPT-4, MM-REACT, BLIP-2, GPT-4	2023
MM-Vet [118]	VQA (open)	$[I, Q]$	Phrases/ Free-Form Response	200	218	GPT-4 Score	Advanced	Advanced	✓	Online sources, VCR [119], ChestX-ray14 [120]	2023
MME [13]	VQA (Binary)	$[I, Q]$	Binary	1077	2194	acc.	Advanced	Advanced	✓	COCO	2024
POPE [121]	VQA (Binary)	$[I, Q]$	Binary	40504	-	F1 score	Basic	-		COCO	2024
LLVisionQA [122]	VQA (MC)	$[I, Q, M]$	MC	2990	2990	GPT score	-	-		10 datasets	2023
LLDescribe [122]	VQA (open)	$[I, Q]$	Free-Form Captions	499	499	GPT-4 Score	-	-		10 datasets	2023
QBench-Assessment [122]	VQA (short)	$[I, Q]$	Number	81,284	-	Softmax	-	-		7 datasets	2023

Table 6: **The Summary of Benchmarks.** In the Input column, I denotes image, Q denotes question, C denotes the context, and M denotes the MC options. [†] denotes GPT-4 is involved in label generation. Otherwise, the label is created manually. The Image # and Question # show train, validation, and test split statistics if available. The benchmarks used for performance analysis are underlined.

5.1 Evaluation Benchmarks

The benchmarks are summarized in Table 6. These benchmarks test two main visual capabilities: Perception ability and Reasoning ability. Both abilities are further categorized into basic and advanced, depending on whether they require knowledge beyond the information available from the image itself. Perception is the capability to recognize features and information from visual input. The MLLMs with basic perception capability can capture features such as color, count, and position [101], while those with advanced capability can utilize the knowledge in LLM to recognize image

emotion [12], movie posters, celebrities [13] and so on. Reasoning ability is the capability to make correct judgments through logical reasoning, object relationship understanding, and attribute inference when faced with complex problems. Testing basic reasoning ability involves understanding the complex question [103], while the advanced involves utilizing common sense and prior knowledge in LLM [11, 116].

Apart from visual understanding, language generation capability can be evaluated through tasks requiring free-form output, such as visual question answering (VQA) with open-ended responses and image captioning. While traditional benchmarks evaluate this capability using statistical similarity metrics such as CIDEr and BLEU [110, 111], advanced benchmarks have shifted towards assessing richer and more detailed outputs [8, 28, 118]. For example, some advanced benchmarks incorporate evaluations conducted by GPT-4 [8, 118, 122], offering a qualitative, context-sensitive measure of the models’ ability to produce detailed and accurate content.

Traditional benchmarks are applicable to all three training paradigms, offering a consistent foundation for evaluation. In contrast, advanced benchmarks are widely used in instruction-tuned models within the Single-stage Tuning paradigm [37, 8, 21, 28, 9, 24, 26, 25, 22, 27, 47, 30, 31, 32]. This is because these models can follow instructions and align outputs closely with the tasks defined in the benchmarks.

Various benchmarks have proposed distinct methods to enable evaluation matrices to assess model outputs. For tasks requiring phrase outputs, accuracies are averaged across all combinations of human annotator subsets in VQAv2 [101]. For multiple-choice (MC) tasks, varied post-processing strategies are employed to align outputs with task requirements. For instance, MemVP [36] limits the output length to one for MC tasks, while LLaVA [8] introduces instructions such as: "Answer the question using a single word or phrase" or "Answer with the option’s letter from the given choices directly." However, recent studies [28, 122] indicate that few VLLMs consistently generate outputs in the instructed format. As a result, there is a growing trend to incorporate LLMs into the evaluation process. For instance, MM-Bench [12] utilizes both rule-based and LLM-driven choice extraction methods to identify answers from the generated textual outputs. Additionally, Q-bench [122] develops a GPT-assisted evaluation framework comprising five iterative rounds.

5.2 Single-stage Tuning

Single-stage Tuning contains one pretraining stage without finetuning on downstream tasks. This training approach initially emerged during the VLPM period. Regarding parameter efficiency, pretraining a VLPM demands multiple feedforward processes, leading to a multiplicative increase in trainable parameters as the model scales up. Single-stage Tuning allows models to pretrain only an MI to connect the two modalities in a single training process. Considering the scale of LLMs, this approach is also parameter-efficient. For pertaining, a large number of image-text pairs are used as pretraining data; representative datasets are LAION-5B [123] and 400M [124], COYO-700M [125], Conceptual Captions 3M[126] and 12M [127], SBU [128] and Visual Genome [129]. ESPER [45] suggests employing a training approach that does not require paired domain data, utilizing RL. It leverages the text encoder of CLIP to compute the similarity between LLM-generated text conditioned on an image and the image itself, which serves as the reward signal to align the two modalities. The RL algorithm used to optimize this reward is the clipped version of PPO [87, 130]. In the multimodal context, the reward is calculated as follows:

$$\alpha \left(X_v / \|X_v\| \cdot \text{CLIP-T}(\hat{Y}) / \|\text{CLIP-T}(\hat{Y})\| \right) + \beta, \quad (27)$$

where α and β are fixed normalizing factors.

After pertaining, Single-stage Tuning leverages the pretrained knowledge in LLMs through zero-shot and few-shot learning, unlike VLPMs, which require end-to-end per-task fine-tuning. VLLMs are evaluated by zero-shot or few-shot Visual Question Answering (VQA) and image captioning. Few-shot prompting is a type of in-context learning [131], which provides example question-answer pairs to the model, and no parameter updates are involved in the process. In most cases, only the Modality Integrator is trainable, while some models involve vision encoders. Overall, Attention-based Abstractors are mostly adopted. The representative works are Q-former [7] and Resampler [16]. MAGMA and Flamingo [16] initiate the idea of utilizing both in-block and Out-of-block Integrators [44].

As shown in Table 7, the performance of Single-stage Tuning on traditional benchmarks highlights several key findings:

1. **Single-stage Tuning demonstrates limitations for downstream task generalization**, as it shows the lowest average scores among the three paradigms. This approach primarily trains the model on image-text pairs, which restricts the model’s ability to generalize across various downstream tasks. The use of zero-shot learning further limits the performance, as the model lacks task-specific knowledge.
2. **Efficient architectural design achieves a good balance between performance and parameter efficiency**, exemplified by MAPL [18], which achieves the highest efficiency within the paradigm and excels in COCO captions. It further reduces the parameter of training only the MI by the efficient resampler design, projecting down and up the

Model	LLM	Trainable	Finetune Technique	Para #	Para %	VQAv2	OKVQA	GQA	COCO	SQA-IMG	TextVQA
Single Stage Training											
<u>Frozen</u> [6]	GPT2-like 1.5B	Linear	-	40.3M	0.64%	48.4	19.6	-	-	-	-
ClipCap [17]	GPT-2 1.5B	Resampler	-	43M	-	-	-	-	113.08	-	-
MAGMA [44]	GPT-J 6B	Linear Projector + Bottleneck Adapter	-	-	-	61.5	40.3	49.6	57	-	-
<u>Flamingo</u> [16]	Chinchilla	Resampler + Attention-based Adapter	-	-	-	-	44.7	-	79.4	-	31.8
MAPL [18]	GPT-J 6B	Resampler	-	3.4M	0.05%	43.51	18.27	-	125.2	-	10.99
ESPER [45]	GPT-2 117M	MLP 2x	-	8M	2.6%	-	-	-	78.2	-	-
BLIP-2 [7]	OPT 6.7B	Q-Former + Linear	-	108M	1.38%	52.6	36.4	36.4	-	-	-
						<u>51.5</u>	<u>31.9</u>	<u>43</u>	<u>93.67</u>		<u>21.3</u>
Two-stage Training											
<u>Flamingo</u> [16]	Chinchilla	Resampler + Attention-based Adapter	Per-task	-	-	82.1	-	-	138.1	-	54.1
LLaMA-Adapter [37]	LLaMA	Linear + Adaptive Prefix	Instruction Tuning (T+V)	1.8M	-	-	-	-	-	80.32	-
ESPER [45]	GPT-2 117M	MLP 2x	Per-task	8M	2.6%	-	-	-	103.1	-	-
LLaVA [8]	LLaMA	Linear + LoRA	Instruction Tuning (V)	4.4M	-	-	-	-	-	90.28	-
MiniGPT4 [21]	Vicuna	Linear	Instruction Tuning (V)	-	-	-	-	32.2	-	-	-
BLIP-2 [7]	OPT6.7B	Q-Former + Linear	Per-task	1.1B	14%	82.19	-	-	145.2	-	-
LLava 1.5 [25]	Vicuna v1.5	MLP+LoRA	Instruction Tuning (V)	0.3B	4.61%	79.1	-	63	-	68.4	58.2
		MLP+DoRA		0.3B	4.63%	78.6	-	62.9	-	-	-
CogVLM-Chat [22]	Vicuna-v1.5	MI+VE	Multi-task Learning + Instruction Tuning (V)	-	-	82.3	64.8	-	-	91.2	70.4
MobileVLM [30]	MobileLLaMA 2.7B	Convolution + Small LLM	instruction tuning (V)	2.71B	-	-	-	59	-	61	47.5
		Convolution + LoRA		0.2B	7.41%	-	-	58.4	-	59.0	46.7
MobileVLM v2 [31]	MobileLLaMA 2.7B	Convolution + Small LLM	Multi-task Learning + Instruction Tuning (V)	2.7B	-	-	-	61.1	-	70.0	57.5
<u>VL-Mamba</u> [32]	Mamba LLM-2.8B	VSS +Small LLM	Instruction Tuning (V)	-	-	76.6	-	56.2	-	65.4	48.9
						<u>80.1</u>	<u>64.8</u>	<u>56.1</u>	<u>141.65</u>	<u>76.1</u>	<u>55.82</u>
Direct Adaptation											
VL-Adapter [33]	T5 base 220M	Linear + Bottleneck Adapter	Multi-task Learning	-	7.98%	66.99 [†]	-	56.36[†]	111.85 [†]	-	-
<u>PromptFusion</u> [35]	GPT3 175B	Prompt	Per-task	15K	-	34.1	-	-	-	-	-
LST [38]	T5 base 220M	Linear + Attention-based Adapter	Multi-task Learning	-	7.46%	67.22[†]	-	56.37[†]	115.05 [†]	-	-
eP-ALM [34]	OPT 2.7B	Linear	Per-task	4.2M	-	54.89	-	42.91	111.63	-	-
LaVIN [41]	LLaMA	Linear + Bottleneck Adapter	Instruction Tuning (T+V)	3.8M	-	-	-	-	-	74.52 [†]	-
VL-PET [40]	T5 base 220M	Linear + Bottleneck Adapter	Multi-task Learning	-	7.31%	67[†]	-	55.97 [†]	122.45[†]	-	-
MemVP [36]	LLaMA	Linear	Per-task	3.9M	-	-	-	-	-	92.36[†]	-
	T5 base 220M	-	-	-	7.23%	65.7	-	56	120.8	-	-
						<u>59.3</u>	-	<u>53.5</u>	<u>116.4</u>	<u>83.44</u>	-

Table 7: **Performance on Traditional Benchmarks.** [†] denotes the replicated results. Others are collected from the papers or GitHub repositories. Underlined numbers are the average of each paradigm on each benchmark. Numbers in **bold** are the best results among all paradigms. Numbers in **blue** background are the best results within each paradigm. Numbers in **pink** background are the second-best results within each paradigm. The LLMs are 7B unless otherwise specified.

input and out of the original resampler structure.

3. **The simultaneous use of In-block and Out-of-Block Integrators proves effective**, as demonstrated by MAGMA [44] and Flamingo [16], which achieve top performance on two benchmarks each. The In-block structures are Bottleneck Adapters and Attention-based Adapters, respectively. This strategy is further applied in the Direct Adaptation paradigm.

4. **Lack of Convolution-based Abstractor.** Designing a lightweight MI becomes crucial when it is the only tunable module in the whole training process. The advantages and drawbacks of three types of Out-of-block Integrators are summarized in Table 5, inspired by [47]. Overall, among the Out-of-block Integrators, the linear mapping and the convolutional structure are usually more efficient than attention-based integrators. Moreover, convolutional structures have higher adaptability than Dense Integrator. However, there is a lack of initiatives to tune only the Convolution-based Abstractors.

5.3 Two-stage Tuning

Two-stage Tuning refers to the pretraining and fine-tuning process. The pretraining stage is similar to Single-stage Tuning, with the goal of aligning the visual feature with the LLM. In addition to the common datasets used in Single-

stage Tuning, CC-595K filtered by Liu et al. [8] from CC3M [126] and ShareGPT4V-PT [132] with more fine-grained captions are utilized.

The fine-tuning techniques used in Two-stage Tuning paradigm includes per-task or multi-task learning, instruction tuning and RL, which are introduced in Section 2.3. In this training paradigm, MTL is concurrently adopted with instruction tuning, as they address different aspects of training. MTL depends on whether the training data includes multiple tasks with different output formats, while instruction tuning depends on whether instructions are provided during the training process.

Instruction Data	Size	Created by	Format	Source	Characteristics	Time
Text-only						
ShareGPT [133]	-	GPT-4/ GPT-3.5	Multi-turn Conversation	-	A tool to export Chat-GPT History	Dec 2022
SlimOrca [134]	518K	GPT-4/ GPT-3.5	Single turn Conversation	OpenOrca	-	Jan 2023
Alpaca [135]	52K	GPT-3.5	Single turn Conversation	-	-	Mar 2023
Baize [136]	111.5K	GPT-3.5-turbo	Multi-turn Conversation	-	-	Apr 2023
GPT4-LLM [137]	52K	GPT-4	Single turn Conversation	Alpaca	-	Apr 2023
Multi-modal						
VisDial [138]	1.2M	Visual Dialog Model	Multi-turn Conversation	COCO	The image is revealed to Visual Dialog Model when captioning	Mar 2017
Video-Chat [139]	4K/ 7K	GPT4	Detailed Description/ Multi-turn Conversation	WebVid-10M	-	April 2023
MiniGPT4 [21]	3K	-	Detailed Description	CC, SBU, ALIGN	-	Jun 2023
LRV-Instruction [140]	300k	GPT4	Single turn Conversation	Visual Genome.	Covering 16 vision-and-language tasks and including positive and negative instructions	June 2023
LLAVA [8]	158K	GPT-4	Multi-turn Conversation	COCO	Context: Caption/Box; Response: conversation, detailed description, complex reasoning	July 2023
LLAVA 1.5 [25]	665K	-	-	LLAVA, ShareGPT, VQAv2, GQA, VG, OKVQA, OCRVQA, A-OKVQA, TextCaps, RefCOCO	-	Oct 2023
ShareGPT4V [132]	100K	GPT4-Vision	Detailed Description	COCO, LAION, CC-3M, and SBU, SAM, TextCaps, WikiArt, web-crawled data	The image is revealed to LLMs when captioning.	Nov 2023
LLAVAR [141]	16K	GPT-4	Multi-turn Conversation	LAION	-	Jun 2024

Table 8: Summary of Instruction Tuning Data.

Model	LLM	Trainable	Para #	PT/FT Size	POPE	MM-Bench	MM-Vet	MME	MME_P	SEED	SEED_1	LLaVA-Bench-Wild
LLaMA-Adapter [37]	LLaMA 7B	Linear + Adaptive Prefix	1.8M	-	-	-	-	-	973	-	-	-
LLaVA [8]	LLaMA-2-7B-Chat	Linear + LoRA	4.4M	558K/158K	-	-	-	-	-	-	-	62.8
MiniGPT4 [21]	Vicuna	Linear	-	558K/665K	-	24.3	22.1	726	867	-	47.4	-
mPLUG-Owl1 [28]	LLaMA	Resampler + LoRA	-	2.1M/102K	-	46.6	-	967.34	-	34	-	-
LLaMA-AdapterV2 [9]	LLaMA	Linear Projector + Degree-Adaptive Prefix + Bias, Norm	14M	567K/52K	-	41	31.4	1221.6	972.7	-	32.7	-
LLava 1.5 [25]	Vicuna v1.5 7B	MLP+LoRA	-	558K/665K	86.4	66.1	30.2	1476.9	-	60.1	-	67.9
CogVLM-Chat [22]	Vicuna-v1.5	MI+VE	-	1.5B/6M	87.9	77.6	51.1	-	-	72.5	-	77.8
MobileVLM [30]	MobileLLaMA 2.7B	Convolution + Small LLM	2.71B	558K/665K	84.9	59.6	-	1288.9	-	-	-	-
		Convolution + LoRA	201.71 M	558K/665K	84.6	57.0	-	1296.4	-	-	-	-
MobileVLM v2 [31]	MobileLLaMA 2.7B	Convolution + Small LLM	2.7B	1.2M/2.4M	84.7	63.2	-	1440.5	-	-	-	-
VL-Mamba [32]	Mamba LLM-2.8B	VSS +Small LLM	-	558K/665K	84.4	57	32.6	1369.6	-	-	-	-

Table 9: Performance of Two-stage Tuning on Advanced Benchmarks.

Instruction Tuning is adopted to equip VLLM with the ability to understand user intentions and improve generalization ability [83, 8]. The instruction data is built by organizing structured datasets in natural language, the idea of which is brought to the multimodal domain by LLaVA [8]. LLaVA [8] uses image captions and bounding boxes to express visual features to prompt text-only GPT4 to generate three types of instruction data: conversation, detailed description,

and complex reasoning. The datasets for instruction tuning are summarized in Table 8. Another approach to instruction tuning involves using instruction prompts to format the responses generated by the VLLM. In this method, the training data typically consists of detailed descriptions [21, 25, 132], enabling the model to produce outputs that align more closely with the provided instructions.

For RL, Sun et al. [46] applied RLHF in the multimodal domain to eliminate hallucinations of images by language models. RLAIIF [48] applies RL with AI feedback. It uses video instruction data to tune VLLMs, generating responses and preferences to train a reward model.

There are three ways to save computational resources under the Two-stage Tuning setting. Like the other two paradigms, tuning only the Modality Integrator is the most efficient way. Among the works [21, 24, 22, 16, 7, 21], Mini-GPT4 only tunes a single linear layer. For those tuning LLMs in the second stage, LoRA-based Tuning discussed in Section 2.2.3 is an option. mPLUG-OWL1 [28] proposes to employ LoRA [29], and Multimodal-GPT [142] finetunes openFlamingo [3] by adding LoRA into the attention module and FFN module. Inspiring work DoRA [74] shows superior performance over full-finetuning and LoRA [29] in LLaVA v1.5, with tuning 4.63% of the parameters. The other way is to employ small-scale LLMs, as in MobileVLM [30, 31] and VL-Mamba [32].

The availability of code implementations is summarized in Table 10. Table 7 and Table 9 reveal several important insights regarding the performance of Two-stage Tuning on traditional and advanced benchmarks:

1. **The additional stage of tuning improves effectiveness, especially Instruction Tuning.** Overall, Two-stage tuning outperforms the other two paradigms, yielding the best results across five benchmarks. This paradigm achieves the top results in most of the benchmarks, with LLaVA 1.5 [25], utilizing 665K instructional data, securing a top-2 performance ranking. On more advanced benchmarks, both LLaVA 1.5 [25] and COGVLM-chat [22] demonstrate competitive performance, consistently producing top-2 results across the majority of advanced benchmarks.
2. **Training only the MI can be effective, and non-updated LLMs can also achieve good performance.** COGVLM-chat [22] achieves strong results across three VQA benchmarks by training only the linear adapters and the vision encoder without requiring updates to the LLM. Similarly, BLIP2 [7] shows notable performance across two benchmarks, highlighting the effectiveness of the Q-former. LLaMA-Adapter [37] tunes 1.8M parameters while achieving the best results on the MME perception set, demonstrating its comparable capabilities in perception tasks.
3. **Reparameterization techniques demonstrate effectiveness.** LLaVA 1.5 [25], utilizing LoRA and Dora, and exhibits robust performance in GQA, outperforming models that tune the LLM. This illustrates the effectiveness of reparameterization techniques in enhancing the performance of the modality integrator without requiring extensive updates to the base model.
4. **Leveraging small-scale LLMs represents a new approach to saving parameters while maintaining competitive performance.** MobileVLM [30] and VL-Mamba [61] achieve the best scores on MM-VET and MME, respectively, highlighting the potential of small-scale LLMs in achieving competitive performance on multimodal benchmarks.

5.4 Direct Adaptation

Direct Adaptation skips the pretraining process and directly finetunes the model to specific downstream tasks. Although Single-stage Tuning and Direct Adaptation both involve one training phase, the knowledge learned from training is different. Taking the VQA task as an example, for Single-stage Tuning, the model learns from descriptive text associated with the images during pretraining. However, during testing, the models are required to answer questions about seen or new images. For Direct Adaptation, the models are directly trained on the data of QA format but tested on unseen questions.

For the learning paradigm, VL-adapter [33] was the first to propose the use of MTL, followed by LST [38] and VL-PET [40]. VL-PET highlights the importance of MTL in enhancing model performance and minimizing storage requirements. LaVIN [41] was the pioneer in applying instruction tuning to the direct adaptation paradigm.

With reducing parameters as the primary goal, VLLMs adopting Direct Adaptation only train the Modality Integrator. Usually, these models utilize both out-of-block and In-block Integrators. A common measure is to first linearly map the visual embedding to the LLM input dimension and then fuse the visual information with In-block Integrators, which are efficient structures, as discussed in Section 4.2. Besides, LLMs of million-level sizes are more often adopted, such as T5 and Bart serving as benchmark LLMs in VL-Adapter [76], VL-PET [40], LaVIN [41], MemVP [36], LST [38].

Most of the results for Direct Adaptation are reproduced as indicated in Table 7 and Table 11. The reproduced results are a single-run outcome. The performance for LaVIN [41] and MemVP [36] in Table 7 and VL-PET [40] and LST [38] in Table 11 are reproduced using the official code repositories. For other methods, reproductions are based on the LST repository [38]. All experiments are run on A100 GPUs. The performance of Direct Adaptation on traditional benchmarks highlights key observations:

1. **Supervised multi-task fine-tuning proves effective**, as evidenced by significant performance improvements over

Model	Pretraining			Finetuning			UI for Inference	Evaluation Supported Datasets
	Code	Data	Code	LoRA	Data	Instruction Template		
OpenFlamingo [3]	✓	×	✓	-	×	-	×	COCO, Flickr-30K, VQA v2, OK-VQA, TextVQA, VizWiz, Hateful Memes, ImageNet
LLaVA [8]	✓	✓	✓	LoRA/qLoRA	✓	✓	✓	VQAv2, GQA, VisWiz, ScienceQA, TextVQA, POPE, MME, MM-Bench, MMVet, LLaVA-Bench-in-the-Wild
LLaVA 1.5 [25]	✓	✓	✓	LoRA	✓	✓	✓	Same as LLaVA
MiniGPT4 [21]	✓	✓	✓	-	✓	✓	×	RefCOCO, RefCOCO+, RefCOCOg, OKVQA, VIZWIZ, ICONVQA, GQA, VSR, HM
mPLUG-Owl 1 [28]	×	×	✓	LoRA	×	✓	✓	OwlEval
mPLUG-Owl 2 [27]	×	×	✓	LoRA	×	✓	✓	Flickr 30k, COCO, VQA v2, OKVQA, TextVQA, MM-Bench
LLaMA-Adapter v2.1 [9]	✓	×	✓	-	✓	-	✓	MME
Video-LLaMA [24]	✓	✓	✓	-	✓	-	×	×
BLIP-2 [7]	✓	✓	✓	-	✓	-	×	Common datasets
QWEN-VL [26]	×	×	✓	LoRA/qLoRA	×	✓	✓	×
COGVLN [22]	×	×	✓	-	×	-	✓	Captcha Images dataset
Honeybee [47]	✓	✓	✓	×	✓	✓	×	MMB, MME, SEED-Bench, ScienceQA, LLaVABench, MMVet, MMMU, POPE, OwlEval
MobileVLM v1/v2 [30] [31]	✓	✓	✓	LoRA	✓	-	×	GQA, MMBench, MME, POPE, SQA, TextVQA

Table 10: **Code Availability of VLLMs with Two-stage Tuning.** "-" denotes that the column is not applicable to the model.

Method	LLM	Trainable Params %	Tunable Component	Peak Memory	VQAv2	GQA	COCO Captions	NLVR	Average
Direct Adaptation									
Full Fine-Tuning [†]	T5 _{base} 220M	100%	Linear + LLM	37.78G	67.13	56.46	112.42	73.60	77.40
Prompt Tuning [†]	T5 _{base} 220M	1.26%	Linear + Prompt	40.03G	47.64	41.12	96.64	51.17	59.14
LoRA [†]	T5 _{base} 220M	7.54%	Linear + LoRA	29.52G	63.88	52.88	110.75	70.32	74.46
VL-Adapter [†]	T5 _{base} 220M	7.98%	Linear + Bottleneck Adapter	30.06G	66.99	56.36	111.85	73.07	77.07
VL-PET [†] _{Small}	T5 _{base} 220M	4.51%	Linear + Bottleneck Adapter	-	65.7	55.78	119.46	73.45	78.60
VL-PET [†] _{MiddleX}	T5 _{base} 220M	4.50%	Linear + Bottleneck Adapter	-	66.54	56.38	120.10	74.72	79.43
VL-PET [†] _{MiddleY}	T5 _{base} 220M	4.50%	Linear + Bottleneck Adapter	-	65.03	55.71	118.07	72.14	77.74
VL-PET [†] _{Large}	T5 _{base} 220M	7.31%	Linear + Bottleneck Adapter	-	67.04	55.97	122.45	72.93	79.60
LST [†]	T5 _{base} 220M	7.46%	Linear + Attention-based Adapter	15.04G	67.22	56.37	115.05	73.04	77.92
MemVP	T5 _{base} 220M	7.23% ³	Linear	-	65.7	56.0	120.8	-	-

Table 11: **Performance of Direct Adaptation on VQAv2, GQA, and COCO Captions.** [†] denotes the replicated results. The result of MemVP [36] is from the paper, which adopts the per-task adaptation and shows the average result of three runs. Others are multi-task learning and the result of one run. The MemVP trainable parameter % is computed based on the proportion to VL-PET_{Large}.

Single-stage Tuning. Compared to Single-Stage Tuning, despite both involving one training stage, Direct Adaptation demonstrates significant improvements, with average score increases of 7.8, 10.5, and 22.7 on VQAv2, GQA, and COCO benchmarks, respectively. MemVP [36] achieves the best performance on the SQA benchmark among the three paradigms, highlighting its focus on parameter efficiency while maintaining competitive performance.

2. **MI in Direct Adaptation focuses on parameter efficiency while retaining good performance.** The idea of bottleneck adapters has mainly been adopted. As shown in Table 11, most MI trains fewer parameters than LoRA, among which the VL-PET series [40] is the most parameter-efficient, with VL-PET_{Large} achieving the best average result. Notably, most models outperform full fine-tuning in terms of average performance.

3. **Memory efficiency also plays a crucial role.** LST [38] demonstrates its effectiveness by reducing memory usage by over 50%, showcasing the potential for scalable applications.

4. **A trend has emerged to adapt larger-scale LLMs and adopt Instruction Tuning.** In the Direct Adaptation framework, T5 [53] and Bart [62] are utilized as the standard LLMs because of their practical sizes [33, 38, 40, 41, 36]. Furthermore, some attempts are to adapt LLaMA models within this framework [41, 36, 37, 9]. As Instruction Tuning is

effective in Two-stage Tuning, LaVIN [41] instructionally adapts LLaMA without pretraining, outperforming LLaVA1.5 on the SQA benchmark.

6 Conclusion

In this survey, we have investigated the evolution of training paradigms and methodology of integrating vision modalities into LLMs to create VLLMs, focusing on parameter efficiency. We categorized the training paradigms into three types: Single-stage Tuning, Two-stage Tuning, and Direct Adaptation. Each paradigm offers unique advantages and efficiency strategies. Single-stage Tuning, which emerged during the VLPM era, effectively leverages pretrained knowledge in LLMs with small additional training, primarily through a Modality Integrator. However, it does not fully unleash the instruction-following potential of LLMs. Two-stage Tuning introduces an additional phase to enhance zero-shot transfer and user intention understanding, focusing on multi-task learning and instruction tuning. This paradigm employs various strategies to reduce trainable parameters, including selective training of the MI, the incorporation of reparameterization modules, and the employment of small-size LLMs. Despite its resource-intensive nature, this approach significantly improves LLMs’ generalization and reasoning abilities. Direct Adaptation, on the other hand, aims to minimize resource consumption by directly fine-tuning the MI on downstream tasks without pretraining, thus providing a balance between parameter efficiency and performance.

In summary, our review highlights several key takeaways that suggest future directions for research in integrating vision modalities into LLMs: among the evaluated paradigms, Two-stage Tuning demonstrated the highest performance, followed by Direct Adaptation, with Single-stage Tuning showing the lowest performance. Meanwhile, Direct Adaptation primarily focuses on parameter efficiency, indicating that the paradigm shift from Single-stage Tuning to the other two methods holds significant potential. Secondly, instruction tuning has emerged as the most popular fine-tuning technique within the Two-stage Tuning paradigm, and there are new attempts to incorporate it into Direct Adaptation. Thirdly, the efficient design of the MI is crucial across all three paradigms. Direct Adaptation, in particular, has led the way in achieving efficiency. Applying efficient MI designs to larger LLMs is becoming increasingly necessary.

Acknowledgment

The research described in this article has been supported by a grant from the Research Grants Council of the Hong Kong Special Administrative Region, China (R1015-23) and the Faculty Research Grant (SDS24A8) and the Direct Grant (DR25E8) of Lingnan University, Hong Kong.

References

- [1] Yifan Du, Zikang Liu, Junyi Li, and Wayne Xin Zhao. A survey of vision-language pre-trained models. In *Proceedings of the 31st International Joint Conference on Artificial Intelligence (IJCAI)*, pages 5436–5443. AAAI Press, 2022.
- [2] Shukang Yin, Chaoyou Fu, Sirui Zhao, Ke Li, Xing Sun, Tong Xu, and Enhong Chen. A survey on multimodal large language models. *Natl. Sci. Rev.*, 11, 2024.
- [3] Anas Awadalla, Irena Gao, Josh Gardner, Jack Hessel, Yusuf Hanafy, Wanrong Zhu, Kalyani Marathe, Yonatan Bitton, Samir Gadre, Shiori Sagawa, Jenia Jitsev, Simon Kornblith, Pang Wei Koh, Gabriel Ilharco, Mitchell Wortsman, and Ludwig Schmidt. Openflamingo: An open-source framework for training large autoregressive vision-language models. *arXiv preprint arXiv:2308.01390*, 2023.
- [4] Junnan Li, Dongxu Li, Caiming Xiong, and Steven Hoi. BLIP: Bootstrapping language-image pre-training for unified vision-language understanding and generation. In *Proceedings of the 39th International Conference on Machine Learning (ICML)*, pages 12888–12900. JMLR, 2022.
- [5] Jiahui Yu, Zirui Wang, Vijay Vasudevan, Legg Yeung, Mojtaba Seyedhosseini, and Yonghui Wu. CoCa: Contrastive captioners are image-text foundation models. *Transact. Mach. Learn. Res.*, 2022.
- [6] Maria Tsimpoukelli, Jacob L Menick, Serkan Cabi, SM Eslami, Oriol Vinyals, and Felix Hill. Multimodal few-shot learning with frozen language models. In *Proceedings of the 35th Annual Conference on Neural Information Processing Systems (NeurIPS)*, volume 34, pages 200–212. Curran Associates, Inc., 2021.
- [7] Junnan Li, Dongxu Li, Silvio Savarese, and Steven Hoi. BLIP-2: Bootstrapping language-image pre-training with frozen image encoders and large language models. In *Proceedings of the 40th International Conference on Machine Learning (ICML)*, pages 19730–19742. JMLR, 2023.

- [8] Haotian Liu, Chunyuan Li, Qingyang Wu, and Yong Jae Lee. Visual instruction tuning. In *Proceedings of the 38th Annual Conference on Neural Information Processing System (NeurIPS)*, volume 36, pages 34892–34916. Curran Associates, Inc., 2024.
- [9] Peng Gao, Jiaming Han, Renrui Zhang, Ziyi Lin, Shijie Geng, Aojun Zhou, Wei Zhang, Pan Lu, Conghui He, Xiangyu Yue, et al. LLaMA-Adapter v2: Parameter-efficient visual instruction model. *arXiv preprint arXiv:2304.15010*, 2023.
- [10] Yueting Yang, Xintong Zhang, and Wenjuan Han. Enhance reasoning ability of visual-language models via large language models. *arXiv preprint arXiv:2305.13267*, 2023.
- [11] Pan Lu, Swaroop Mishra, Tanglin Xia, Liang Qiu, Kai-Wei Chang, Song-Chun Zhu, Oyvind Tafjord, Peter Clark, and Ashwin Kalyan. Learn to explain: Multimodal reasoning via thought chains for science question answering. In *Proceedings of the 36th Annual Conference on Neural Information Processing Systems (NeurIPS)*, volume 35, pages 2507–2521. Curran Associates Inc, 2022.
- [12] Yuan Liu, Haodong Duan, Yuanhan Zhang, Bo Li, Songyang Zhang, Wangbo Zhao, Yike Yuan, Jiaqi Wang, Conghui He, Ziwei Liu, et al. MMBench: Is your multi-modal model an all-around player? *arXiv preprint arXiv:2307.06281*, 2023.
- [13] Chaoyou Fu, Peixian Chen, Yunhang Shen, Yulei Qin, Mengdan Zhang, Xu Lin, Jinrui Yang, Xiawu Zheng, Ke Li, Xing Sun, et al. MME: A comprehensive evaluation benchmark for multimodal large language models. *arXiv preprint arXiv:2306.13394*, 2023.
- [14] Yizhang Jin, Jian Li, Yexin Liu, Tianjun Gu, Kai Wu, Zhengkai Jiang, MUYANG He, Bo Zhao, Xin Tan, Zhenye Gan, et al. Efficient multimodal large language models: A survey. *arXiv preprint arXiv:2405.10739*, 2024.
- [15] Lingling Xu, Haoran Xie, Si-Zhao Joe Qin, Xiaohui Tao, and Fu Lee Wang. Parameter-efficient fine-tuning methods for pretrained language models: A critical review and assessment. *arXiv preprint arXiv:2312.12148*, 2023.
- [16] Jean-Baptiste Alayrac, Jeff Donahue, Pauline Luc, Antoine Miech, Iain Barr, Yana Hasson, Karel Lenc, Arthur Mensch, Katherine Millican, Malcolm Reynolds, et al. Flamingo: A visual language model for few-shot learning. In *Proceedings of the 36th Annual Conference on Neural Information Processing Systems (NeurIPS)*, volume 35, pages 23716–23736. Curran Associates, Inc., 2022.
- [17] Ron Mokady, Amir Hertz, and Amit H Bermano. Clipcap: Clip prefix for image captioning. *arXiv preprint arXiv:2111.09734*, 2021.
- [18] Oscar Mañas, Pau Rodriguez Lopez, Saba Ahmadi, Aida Nematzadeh, Yash Goyal, and Aishwarya Agrawal. MAPL: Parameter-efficient adaptation of unimodal pre-trained models for vision-language few-shot prompting. In *Proceedings of the 17th Conference of the European Chapter of the Association for Computational Linguistics (EACL)*, pages 2523–2548. ACL, 2023.
- [19] Ivona Najdenkoska, Xiantong Zhen, and Marcel Worring. Meta learning to bridge vision and language models for multimodal few-shot learning. In *The 11th International Conference on Learning Representations (ICLR)*. ICLR, 2023.
- [20] Jing Yu Koh, Ruslan Salakhutdinov, and Daniel Fried. Grounding language models to images for multimodal inputs and outputs. In *Proceedings of the 40th International Conference on Machine Learning (ICML)*, pages 17283–17300. JMLR, 2023.
- [21] Deyao Zhu, Jun Chen, Xiaoqian Shen, Xiang Li, and Mohamed Elhoseiny. MiniGPT-4: Enhancing vision-language understanding with advanced large language models. In *Proceedings of the 12th International Conference on Learning Representations (ICLR)*. ICLR, 2024.
- [22] Weihang Wang, Qingsong Lv, Wenmeng Yu, Wenyi Hong, Ji Qi, Yan Wang, Junhui Ji, Zhuoyi Yang, Lei Zhao, Xixuan Song, et al. CogVLM: Visual expert for pretrained language models. *arXiv preprint arXiv:2311.03079*, 2023.
- [23] Antoine Yang, Antoine Miech, Josef Sivic, Ivan Laptev, and Cordelia Schmid. Zero-shot video question answering via frozen bidirectional language models. In *Proceedings of the 36th Annual Conference on Neural Information Processing Systems (NeurIPS)*, volume 35, pages 124–141. Curran Associates, Inc., 2022.
- [24] Hang Zhang, Xin Li, and Lidong Bing. Video-LLaMA: An instruction-tuned audio-visual language model for video understanding. In *Proceedings of the 2023 Conference on Empirical Methods in Natural Language Processing: System Demonstrations (EMNLP)*, pages 543–553. ACL, 2023.
- [25] Haotian Liu, Chunyuan Li, Yuheng Li, and Yong Jae Lee. Improved baselines with visual instruction tuning. In *Proceedings of the IEEE/CVF Conference on Computer Vision and Pattern Recognition (CVPR)*, pages 26296–26306. IEEE, 2024.

- [26] Jinze Bai, Shuai Bai, Yunfei Chu, Zeyu Cui, Kai Dang, Xiaodong Deng, Yang Fan, Wenbin Ge, Yu Han, Fei Huang, et al. Qwen technical report. *arXiv preprint arXiv:2309.16609*, 2023.
- [27] Qinghao Ye, Haiyang Xu, Jiabo Ye, Ming Yan, Anwen Hu, Haowei Liu, Qi Qian, Ji Zhang, and Fei Huang. mPLUG-Owl2: Revolutionizing multi-modal large language model with modality collaboration. In *Proceedings of the 2024 IEEE/CVF Conference on Computer Vision and Pattern Recognition (CVPR)*, pages 13040–13051. IEEE, 2024.
- [28] Qinghao Ye, Haiyang Xu, Guohai Xu, Jiabo Ye, Ming Yan, Yiyang Zhou, Junyang Wang, Anwen Hu, Pengcheng Shi, Yaya Shi, et al. mPLUG-Owl: Modularization empowers large language models with multimodality. *arXiv preprint arXiv:2304.14178*, 2023.
- [29] Edward J Hu, yelong shen, Phillip Wallis, Zeyuan Allen-Zhu, Yanzhi Li, Shean Wang, Lu Wang, and Weizhu Chen. LoRA: Low-rank adaptation of large language models. In *Proceedings of the 10th International Conference on Learning Representations (ICLR)*. ICLR, 2022.
- [30] Xiangxiang Chu, Limeng Qiao, Xinyang Lin, Shuang Xu, Yang Yang, Yiming Hu, Fei Wei, Xinyu Zhang, Bo Zhang, Xiaolin Wei, et al. MobileVLM: A fast, strong and open vision language assistant for mobile devices. *arXiv preprint arXiv:2312.16886*, 2023.
- [31] Xiangxiang Chu, Limeng Qiao, Xinyu Zhang, Shuang Xu, Fei Wei, Yang Yang, Xiaofei Sun, Yiming Hu, Xinyang Lin, Bo Zhang, et al. MobileVLM v2: Faster and stronger baseline for vision language model. *arXiv preprint arXiv:2402.03766*, 2024.
- [32] Yanyuan Qiao, Zheng Yu, Longteng Guo, Sihan Chen, Zijia Zhao, Mingzhen Sun, Qi Wu, and Jing Liu. VL-Mamba: Exploring state space models for multimodal learning. *arXiv preprint arXiv:2403.13600*, 2024.
- [33] Yi-Lin Sung, Jaemin Cho, and Mohit Bansal. VL-Adapter: Parameter-efficient transfer learning for vision-and-language tasks. In *Proceedings of the 2022 IEEE/CVF Conference on Computer Vision and Pattern Recognition (CVPR)*, pages 5227–5237. IEEE, 2022.
- [34] Mustafa Shukor, Corentin Dancette, and Matthieu Cord. eP-ALM: Efficient perceptual augmentation of language models. In *Proceedings of the 2023 IEEE/CVF International Conference on Computer Vision (ICCV)*, pages 22056–22069. IEEE, 2023.
- [35] Sheng Liang, Mengjie Zhao, and Hinrich Schuetze. Modular and parameter-efficient multimodal fusion with prompting. In *Findings of the Association for Computational Linguistics: ACL 2022*, pages 2976–2985. ACL, 2022.
- [36] Shibo Jie, Yehui Tang, Ning Ding, Zhi-Hong Deng, Kai Han, and Yunhe Wang. Memory-space visual prompting for efficient vision-language fine-tuning. In *Proceedings of the 41th International Conference on Machine Learning (ICML)*. JMLR, 2024.
- [37] Renrui Zhang, Jiaming Han, Chris Liu, Aojun Zhou, Pan Lu, Yu Qiao, Hongsheng Li, and Peng Gao. LLaMA-Adapter: Efficient fine-tuning of large language models with zero-initialized attention. In *Proceedings of the 12th International Conference on Learning Representations (ICLR)*. ICLR, 2024.
- [38] Yi-Lin Sung, Jaemin Cho, and Mohit Bansal. LST: Ladder side-tuning for parameter and memory efficient transfer learning. In *Proceedings of the 36th Annual Conference on Neural Information Processing Systems (NeurIPS)*, volume 35, pages 12991–13005. Curran Associates, Inc., 2022.
- [39] Tian Liang, Jing Huang, Ming Kong, Luyuan Chen, and Qiang Zhu. Querying as Prompt: Parameter-efficient learning for multimodal language model. In *Proceedings of the 2024 IEEE/CVF Conference on Computer Vision and Pattern Recognition (CVPR)*, pages 26855–26865, 2024.
- [40] Zi-Yuan Hu, Yanyang Li, Michael R Lyu, and Liwei Wang. VL-PET: Vision-and-language parameter-efficient tuning via granularity control. In *Proceedings of the 2023 IEEE/CVF International Conference on Computer Vision (ICCV)*, pages 3010–3020. IEEE, 2023.
- [41] Gen Luo, Yiyi Zhou, Tianhe Ren, Shengxin Chen, Xiaoshuai Sun, and Rongrong Ji. Cheap and Quick: Efficient vision-language instruction tuning for large language models. In *Proceedings of the 38th Annual Conference on Neural Information Processing Systems (NeurIPS)*, volume 36. Curran Associates, Inc., 2024.
- [42] Google scholar. <https://scholar.google.com/>, accessed 3 February 2025.
- [43] CCF recommended list of international conferences and periodicals. <https://ccf.atom.im/>, accessed 3 February 2025.
- [44] Constantin Eichenberg, Sidney Black, Samuel Weinbach, Letitia Parcalabescu, and Anette Frank. MAGMA – Multimodal augmentation of generative models through adapter-based finetuning. In *Findings of the Association for Computational Linguistics: EMNLP 2022*, pages 2416–2428. ACL, 2022.

- [45] Youngjae Yu, Jiwan Chung, Heeseung Yun, Jack Hessel, Jae Sung Park, Ximing Lu, Rowan Zellers, Prithviraj Ammanabrolu, Ronan Le Bras, Gunhee Kim, and Yejin Choi. Fusing pre-trained language models with multimodal prompts through reinforcement learning. In *Proceedings of the 2023 IEEE/CVF Conference on Computer Vision and Pattern Recognition (CVPR)*, pages 10845–10856. IEEE, 2023.
- [46] Zhiqing Sun, Sheng Shen, Shengcao Cao, Haotian Liu, Chunyuan Li, Yikang Shen, Chuang Gan, Liangyan Gui, Yu-Xiong Wang, Yiming Yang, Kurt Keutzer, and Trevor Darrell. Aligning large multimodal models with factually augmented RLHF. In *Findings of the Association for Computational Linguistics: ACL 2024*, pages 13088–13110. ACL, 2024.
- [47] Junbum Cha, Wooyoung Kang, Jonghwan Mun, and Byungseok Roh. Honeybee: Locality-enhanced projector for multimodal LLM. In *Proceedings of the 2024 IEEE/CVF Conference on Computer Vision and Pattern Recognition (CVPR)*, pages 13817–13827. IEEE, 2024.
- [48] Daechul Ahn, Yura Choi, Youngjae Yu, Dongyeop Kang, and Jonghyun Choi. Tuning large multimodal models for videos using reinforcement learning from AI feedback. In *Proceedings of the 62nd Annual Meeting of the Association for Computational Linguistics (ACL)*, pages 923–940. Association for Computational Linguistics, 2024.
- [49] Feilong Chen, Minglun Han, Haozhi Zhao, Qingyang Zhang, Jing Shi, Shuang Xu, and Bo Xu. X-LLM: Bootstrapping advanced large language models by treating multi-modalities as foreign languages. *arXiv preprint arXiv:2305.04160*, 2023.
- [50] Ashish Vaswani, Noam Shazeer, Niki Parmar, Jakob Uszkoreit, Llion Jones, Aidan N Gomez, Łukasz Kaiser, and Illia Polosukhin. Attention is all you need. In *Proceedings of the 31st Annual Conference on Neural Information Processing Systems (NeurIPS)*, volume 30. Curran Associates, Inc., 2017.
- [51] Yinhan Liu, Myle Ott, Naman Goyal, Jingfei Du, Mandar Joshi, Danqi Chen, Omer Levy, Mike Lewis, Luke Zettlemoyer, and Veselin Stoyanov. RoBERTa: A robustly optimized bert pretraining approach. *arXiv preprint arXiv:1907.11692*, 2019.
- [52] Pengcheng He, Xiaodong Liu, Jianfeng Gao, and Weizhu Chen. DeBERTa: Decoding-enhanced BERT with disentangled attention. In *Proceedings of the 9th International Conference on Learning Representations (ICLR)*. ICLR, 2021.
- [53] Colin Raffel, Noam Shazeer, Adam Roberts, Katherine Lee, Sharan Narang, Michael Matena, Yanqi Zhou, Wei Li, and Peter J Liu. Exploring the limits of transfer learning with a unified text-to-text transformer. *J. Mach. Learn. Res.*, 21(140):1–67, 2020.
- [54] Mike Lewis, Yinhan Liu, Naman Goyal, Marjan Ghazvininejad, Abdelrahman Mohamed, Omer Levy, Veselin Stoyanov, and Luke Zettlemoyer. BART: Denoising sequence-to-sequence pre-training for natural language generation, translation, and comprehension. In *Proceedings of the 58th Annual Meeting of the Association for Computational Linguistics (ACL)*, pages 7871–7880. ACL, 2020.
- [55] Hugo Touvron, Thibaut Lavril, Gautier Izacard, Xavier Martinet, Marie-Anne Lachaux, Timothée Lacroix, Baptiste Rozière, Naman Goyal, Eric Hambro, Faisal Azhar, et al. LLaMA: Open and efficient foundation language models. *arXiv preprint arXiv:2302.13971*, 2023.
- [56] The Vicuna Team. VICUNA: An open-source chatbot impressing gpt-4 with 90% chatgpt quality. <https://lmsys.org/blog/2023-03-30-vicuna/>, March 2023.
- [57] Susan Zhang, Stephen Roller, Naman Goyal, Mikel Artetxe, Moya Chen, Shuohui Chen, Christopher Dewan, Mona Diab, Xian Li, Xi Victoria Lin, et al. OPT: Open pre-trained transformer language models. *arXiv preprint arXiv:2205.01068*, 2022.
- [58] Luciano Floridi and Massimo Chiriatti. GPT-3: Its nature, scope, limits, and consequences. *Minds and Machines*, 30:681–694, 2020.
- [59] Josh Achiam, Steven Adler, Sandhini Agarwal, Lama Ahmad, Ilge Akkaya, Florencia Leoni Aleman, Diogo Almeida, Janko Altenschmidt, Sam Altman, Shyamal Anadkat, et al. GPT-4 technical report. *arXiv preprint arXiv:2303.08774*, 2023.
- [60] Team GLM, Aohan Zeng, Bin Xu, Bowen Wang, Chenhui Zhang, Da Yin, Diego Rojas, Guanyu Feng, Hanlin Zhao, Hanyu Lai, et al. ChatGLM: A family of large language models from GLM-130B to GLM-4 all tools. *arXiv preprint arXiv:2406.12793*, 2024.
- [61] Albert Gu and Tri Dao. Mamba: Linear-time sequence modeling with selective state spaces. *arXiv preprint arXiv:2312.00752*, 2023.

- [62] Hyung Won Chung, Le Hou, Shayne Longpre, Barret Zoph, Yi Tay, William Fedus, Yunxuan Li, Xuezhi Wang, Mostafa Dehghani, Siddhartha Brahma, et al. Scaling instruction-finetuned language models. *J. Mach. Learn. Res.*, 25(70):1–53, 2024.
- [63] Tom Brown, Benjamin Mann, Nick Ryder, Melanie Subbiah, Jared D Kaplan, Prafulla Dhariwal, Arvind Neelakantan, Pranav Shyam, Girish Sastry, Amanda Askell, et al. Language models are few-shot learners. In *Proceedings of the 34th Annual Conference on Neural Information Processing Systems (NeurIPS)*, volume 33, pages 1877–1901. Curran Associates, Inc., 2020.
- [64] Ben Wang and Aran Komatsuzaki. GPT-J-6B: A 6 Billion Parameter Autoregressive Language Model [software]. <https://github.com/kingoflolz/mesh-transformer-jax>, May 2021.
- [65] Jordan Hoffmann, Sebastian Borgeaud, Arthur Mensch, Elena Buchatskaya, Trevor Cai, Eliza Rutherford, Diego de Las Casas, Lisa Anne Hendricks, Johannes Welbl, Aidan Clark, Thomas Hennigan, Eric Noland, Katherine Millican, George van den Driessche, Bogdan Damoc, Aurelia Guy, Simon Osindero, Karén Simonyan, Erich Elsen, Oriol Vinyals, Jack Rae, and Laurent Sifre. An empirical analysis of compute-optimal large language model training. In *The 36th Annual Conference on Neural Information Processing Systems (NeurIPS)*, volume 35, pages 30016–30030. Curran Associates, Inc., 2022.
- [66] Mosaic AI Research. Introducing MPT-7B: A New Standard for Open-Source, Commercially Usable LLMs [software]. <https://www.databricks.com/blog/mpt-7b>, May 2023.
- [67] Together.ai. Releasing 3B and 7B RedPajama-INCITE family of models including base, instruction-tuned & chat models [software]. <https://www.together.ai/blog/redpajama-models-v1>, May 2023.
- [68] Hugo Touvron, Louis Martin, Kevin Stone, Peter Albert, Amjad Almahairi, Yasmine Babaei, Nikolay Bashlykov, Soumya Batra, Prajjwal Bhargava, Shruti Bhosale, et al. LLaMA 2: Open foundation and fine-tuned chat models. *arXiv preprint arXiv:2307.09288*, 2023.
- [69] Noam Shazeer. Glu variants improve transformer. *arXiv preprint arXiv:2002.05202*, 2020.
- [70] Xiang Lisa Li and Percy Liang. Prefix-Tuning: Optimizing continuous prompts for generation. In *Proceedings of the 59th Annual Meeting of the Association for Computational Linguistics and the 11th International Joint Conference on Natural Language Processing (ACL)*, pages 4582–4597. ACL, 2021.
- [71] Brian Lester, Rami Al-Rfou, and Noah Constant. The power of scale for parameter-efficient prompt tuning. In *Proceedings of the 2021 Conference on Empirical Methods in Natural Language Processing (EMNLP)*, pages 3045–3059. ACL, 2021.
- [72] Neil Houlsby, Andrei Giurgiu, Stanislaw Jastrzebski, Bruna Morrone, Quentin De Laroussilhe, Andrea Gesmundo, Mona Attariyan, and Sylvain Gelly. Parameter-efficient transfer learning for NLP. In *Proceedings of the 36th International Conference on Machine Learning (ICML)*, pages 2790–2799. JMLR, 2019.
- [73] Tim Dettmers, Artidoro Pagnoni, Ari Holtzman, and Luke Zettlemoyer. QLoRA: Efficient finetuning of quantized lms. In *Proceedings of the 37th Annual Conference on Neural Information Processing Systems (NeurIPS)*, volume 36, pages 10088–10115. Curran Associates, Inc., 2023.
- [74] Shih-Yang Liu, Chien-Yi Wang, Hongxu Yin, Pavlo Molchanov, Yu-Chiang Frank Wang, Kwang-Ting Cheng, and Min-Hung Chen. DoRA: Weight-decomposed low-rank adaptation. *arXiv preprint arXiv:2402.09353*, 2024.
- [75] Menglin Jia, Luming Tang, Bor-Chun Chen, Claire Cardie, Serge Belongie, Bharath Hariharan, and Ser-Nam Lim. Visual prompt tuning. In *Proceedings of the 17th European Conference on Computer Vision (ECCV)*, pages 709–727. Springer, 2022.
- [76] Zhaojiang Lin, Andrea Madotto, and Pascale Fung. Exploring versatile generative language model via parameter-efficient transfer learning. In *Findings of the Association for Computational Linguistics: EMNLP 2020*, pages 441–459. ACL, 2020.
- [77] Junxian He, Chunting Zhou, Xuezhe Ma, Taylor Berg-Kirkpatrick, and Graham Neubig. Towards a unified view of parameter-efficient transfer learning. In *The 10th International Conference on Learning Representations (ICLR)*. ICLR, 2022.
- [78] Alexandra Chronopoulou, Matthew Peters, Alexander Fraser, and Jesse Dodge. AdapterSoup: Weight averaging to improve generalization of pretrained language models. In *Findings of the Association for Computational Linguistics: EACL 2023*, pages 2054–2063. ACL, 2023.
- [79] Xiaodong Liu, Pengcheng He, Weizhu Chen, and Jianfeng Gao. Multi-task deep neural networks for natural language understanding. *arXiv preprint arXiv:1901.11504*, 2019.
- [80] Rich Caruana. Multitask learning. *Mach. Learn.*, 28:41–75, 1997.

- [81] Zhihan Zhang, Wenhao Yu, Mengxia Yu, Zhichun Guo, and Meng Jiang. A survey of multi-task learning in natural language processing: Regarding task relatedness and training methods. In *Proceedings of the 17th Conference of the European Chapter of the Association for Computational Linguistics (EACL)*, pages 943–956. ACL, May 2023.
- [82] Wenna Lai, Haoran Xie, Guandong Xu, and Qing Li. Multi-task learning with llms for implicit sentiment analysis: Data-level and task-level automatic weight learning. *arXiv preprint arXiv:2412.09046*, 2024.
- [83] Jason Wei, Maarten Bosma, Vincent Zhao, Kelvin Guu, Adams Wei Yu, Brian Lester, Nan Du, Andrew M. Dai, and Quoc V Le. Finetuned language models are zero-shot learners. In *Proceedings of the 10th International Conference on Learning Representations (ICLR)*, 2022.
- [84] Long Ouyang, Jeffrey Wu, Xu Jiang, Diogo Almeida, Carroll Wainwright, Pamela Mishkin, Chong Zhang, Sandhini Agarwal, Katarina Slama, Alex Ray, et al. Training language models to follow instructions with human feedback. In *Proceedings of the 36th Annual Conference on Neural Information Processing Systems (NeurIPS)*, volume 35, pages 27730–27744. Curran Associates, Inc., 2022.
- [85] Yuntao Bai, Saurav Kadavath, Sandipan Kundu, Amanda Askell, Jackson Kernion, Andy Jones, Anna Chen, Anna Goldie, Azalia Mirhoseini, Cameron McKinnon, et al. Constitutional AI: Harmlessness from ai feedback. *arXiv preprint arXiv:2212.08073*, 2022.
- [86] Daya Guo, Dejian Yang, Haowei Zhang, Junxiao Song, Ruoyu Zhang, Runxin Xu, Qihao Zhu, Shirong Ma, Peiyi Wang, Xiao Bi, et al. DeepSeek-R1: Incentivizing reasoning capability in LLMs via reinforcement learning. *arXiv preprint arXiv:2501.12948*, 2025.
- [87] John Schulman, Filip Wolski, Prafulla Dhariwal, Alec Radford, and Oleg Klimov. Proximal policy optimization algorithms. *arXiv preprint arXiv:1707.06347*, 2017.
- [88] Tianyu Yu, Yuan Yao, Haoye Zhang, Taiwen He, Yifeng Han, Ganqu Cui, Jinyi Hu, Zhiyuan Liu, Hai-Tao Zheng, Maosong Sun, et al. RLHF-V: Towards trustworthy MLLMs via behavior alignment from fine-grained correctional human feedback. In *Proceedings of the IEEE/CVF Conference on Computer Vision and Pattern Recognition (CVPR)*, pages 13807–13816. IEEE, 2024.
- [89] Alec Radford, Jong Wook Kim, Chris Hallacy, Aditya Ramesh, Gabriel Goh, Sandhini Agarwal, Girish Sastry, Amanda Askell, Pamela Mishkin, Jack Clark, et al. Learning transferable visual models from natural language supervision. In *Proceedings of the 38th International Conference on Machine Learning (ICML)*, pages 8748–8763. JMLR, 2021.
- [90] Alexey Dosovitskiy, Lucas Beyer, Alexander Kolesnikov, Dirk Weissenborn, Xiaohua Zhai, Thomas Unterthiner, Mostafa Dehghani, Matthias Minderer, Georg Heigold, Sylvain Gelly, Jakob Uszkoreit, and Neil Houlsby. An image is worth 16x16 words: Transformers for image recognition at scale. In *Proceedings of the 9th International Conference on Learning Representations (ICLR)*. ICLR, 2021.
- [91] Andy Brock, Soham De, Samuel L Smith, and Karen Simonyan. High-performance large-scale image recognition without normalization. In *Proceedings of the 38th International Conference on Machine Learning (ICML)*, pages 1059–1071. JMLR, 2021.
- [92] Xiaohua Zhai, Alexander Kolesnikov, Neil Houlsby, and Lucas Beyer. Scaling vision transformers. In *Proceedings of the 2022 IEEE/CVF Conference on Computer Vision and Pattern Recognition (CVPR)*, pages 12104–12113. IEEE, 2022.
- [93] Mehdi Cherti, Romain Beaumont, Ross Wightman, Mitchell Wortsman, Gabriel Ilharco, Cade Gordon, Christoph Schuhmann, Ludwig Schmidt, and Jenia Jitsev. Reproducible scaling laws for contrastive language-image learning. In *Proceedings of the 2023 IEEE/CVF Conference on Computer Vision and Pattern Recognition (CVPR)*, pages 2818–2829. IEEE, 2023.
- [94] Quan Sun, Yuxin Fang, Ledell Wu, Xinlong Wang, and Yue Cao. EVA-CLIP: Improved training techniques for clip at scale. *arXiv preprint arXiv:2303.15389*, 2023.
- [95] Gabriel Ilharco, Mitchell Wortsman, Ross Wightman, Cade Gordon, Nicholas Carlini, Rohan Taori, Achal Dave, Vaishaal Shankar, Hongseok Namkoong, John Miller, Hannaneh Hajishirzi, Ali Farhadi, and Ludwig Schmidt. OpenCLIP [software], July 2021. Zenodo.
- [96] Kaiming He, Xiangyu Zhang, Shaoqing Ren, and Jian Sun. Deep residual learning for image recognition. In *Proceedings of the 2016 IEEE Conference on Computer Vision and Ptern Recognition (CVPR)*, pages 770–778. IEEE, 2016.
- [97] Jack Merullo, Louis Castricato, Carsten Eickhoff, and Ellie Pavlick. Linearly mapping from image to text space. In *Proceedings of the 11th International Conference on Learning Representations (ICLR)*. ICLR, 2023.

- [98] Xizhou Zhu, Weijie Su, Lewei Lu, Bin Li, Xiaogang Wang, and Jifeng Dai. Deformable DETR: Deformable transformers for end-to-end object detection. In *Proceedings of the 9th International Conference on Learning Representations (ICLR)*. ICLR, 2021.
- [99] Saining Xie, Ross Girshick, Piotr Dollár, Zhuowen Tu, and Kaiming He. Aggregated residual transformations for deep neural networks. In *Proceedings of the 2017 IEEE Conference on Computer Vision and Pattern Recognition (CVPR)*, pages 1492–1500. IEEE, 2017.
- [100] Xiangxiang Chu, Zhi Tian, Bo Zhang, Xinlong Wang, and Chunhua Shen. Conditional positional encodings for vision transformers. In *Proceedings of the 11th International Conference on Learning Representations (ICLR)*. ICLR, 2023.
- [101] Stanislaw Antol, Aishwarya Agrawal, Jiasen Lu, Margaret Mitchell, Dhruv Batra, C Lawrence Zitnick, and Devi Parikh. VQA: Visual question answering. In *Proceedings of the 2015 IEEE International Conference on Computer Vision (ICCV)*, pages 2425–2433. IEEE, 2015.
- [102] Kenneth Marino, Mohammad Rastegari, Ali Farhadi, and Roozbeh Mottaghi. OK-VQA: A visual question answering benchmark requiring external knowledge. In *Proceedings of the 2019 Conference on Computer Vision and Pattern Recognition (CVPR)*. IEEE, 2019.
- [103] Drew A Hudson and Christopher D Manning. GQA: A new dataset for real-world visual reasoning and compositional question answering. In *Proceedings of the IEEE/CVF Conference on Computer Vision and Pattern Recognition (CVPR)*, pages 6700–6709. IEEE, 2019.
- [104] Danna Gurari, Qing Li, Abigale Stangl, Anhong Guo, Chi Lin, Kristen Grauman, Jiebo Luo, and Jeffrey P. Bigham. VizWiz Grand Challenge: Answering visual questions from blind people. In *Proceedings of the 2018 IEEE/CVF Conference on Computer Vision and Pattern Recognition (CVPR)*, pages 3608–3617. IEEE, 2018.
- [105] Amanpreet Singh, Vivek Natarajan, Meet Shah, Yu Jiang, Xinlei Chen, Dhruv Batra, Devi Parikh, and Marcus Rohrbach. Towards VQA models that can read. In *Proceedings of the 2019 IEEE/CVF Conference on Computer Vision and Pattern Recognition (CVPR)*, pages 8309–8318. IEEE, 2019.
- [106] Ivan Krasin, Tom Duerig, Neil Alldrin, Vittorio Ferrari, Sami Abu-El-Haija, Alina Kuznetsova, Hassan Rom, Jasper Uijlings, Stefan Popov, Andreas Veit, et al. Openimages: A public dataset for large-scale multi-label and multi-class image classification [dataset], 2017.
- [107] Anand Mishra, Shashank Shekhar, Ajeet Kumar Singh, and Anirban Chakraborty. OCR-VQA: Visual question answering by reading text in images. In *Proceedings of the 15th International Conference on Document Analysis and Recognition (ICDAR)*, pages 947–952. IEEE, 2019.
- [108] Brian Kenji Iwana, Syed Tahseen Raza Rizvi, Sheraz Ahmed, Andreas Dengel, and Seiichi Uchida. Judging a book by its cover. *arXiv preprint arXiv:1610.09204*, 2016.
- [109] Xinlei Chen, Hao Fang, Tsung-Yi Lin, Ramakrishna Vedantam, Saurabh Gupta, Piotr Dollár, and C Lawrence Zitnick. Microsoft COCO Captions: Data collection and evaluation server. *arXiv preprint arXiv:1504.00325*, 2015.
- [110] Ramakrishna Vedantam, C Lawrence Zitnick, and Devi Parikh. CIDEr: Consensus-based image description evaluation. In *Proceedings of the 2015 IEEE Conference on Computer Vision and Pattern Recognition (CVPR)*, pages 4566–4575. IEEE, 2015.
- [111] Kishore Papineni, Salim Roukos, Todd Ward, and Wei-Jing Zhu. BLEU: A method for automatic evaluation of machine translation. In *Proceedings of the 40th annual meeting of the Association for Computational Linguistics (ACL)*, pages 311–318. ACL, 2002.
- [112] Harsh Agrawal, Karan Desai, Yufei Wang, Xinlei Chen, Rishabh Jain, Mark Johnson, Dhruv Batra, Devi Parikh, Stefan Lee, and Peter Anderson. Nocaps: Novel object captioning at scale. In *Proceedings of the 2019 IEEE/CVF International Conference on Computer Vision (ICCV)*, pages 8948–8957. IEEE, 2019.
- [113] Peter Anderson, Basura Fernando, Mark Johnson, and Stephen Gould. SPICE: Semantic propositional image caption evaluation. In *Proceedings of the 14th European Conference on Computer Vision (ECCV)*, pages 382–398. Springer, 2016.
- [114] Xu Jia, Efstratios Gavves, Basura Fernando, and Tinne Tuytelaars. Guiding the long-short term memory model for image caption generation. In *Proceedings of the 2015 IEEE International Conference on Computer Vision (ICCV)*, page 2407–2415. IEEE Computer Society, 2015.
- [115] Alane Suhr, Mike Lewis, James Yeh, and Yoav Artzi. A corpus of natural language for visual reasoning. In *Proceedings of the 55th Annual Meeting of the Association for Computational Linguistics (ACL)*, pages 217–223. ACL, 2017.

- [116] Bohao Li, Yuying Ge, Yixiao Ge, Guangzhi Wang, Rui Wang, Ruimao Zhang, and Ying Shan. SEED-Bench: Benchmarking multimodal large language models. In *Proceedings of the 2024 IEEE/CVF Conference on Computer Vision and Pattern Recognition (CVPR)*, pages 13299–13308. IEEE, 2024.
- [117] Yizhong Wang, Yeganeh Kordi, Swaroop Mishra, Alisa Liu, Noah A. Smith, Daniel Khashabi, and Hannaneh Hajishirzi. Self-Instruct: Aligning language models with self-generated instructions. In *Proceedings of the 61st Annual Meeting of the Association for Computational Linguistics (ACL)*. ACL, 2023.
- [118] Weihao Yu, Zhengyuan Yang, Linjie Li, Jianfeng Wang, Kevin Lin, Zicheng Liu, Xinchao Wang, and Lijuan Wang. MM-Vet: Evaluating large multimodal models for integrated capabilities. In *Proceedings of the 41st International Conference on Machine Learning (ICML)*. PMLR, 2024.
- [119] Rowan Zellers, Yonatan Bisk, Ali Farhadi, and Yejin Choi. From recognition to cognition: Visual commonsense reasoning. In *Proceedings of the 2019 IEEE/CVF Conference on Computer Vision and Pattern Recognition (CVPR)*, pages 6713–6724. IEEE, 2019.
- [120] Xiaosong Wang, Yifan Peng, Le Lu, Zhiyong Lu, Mohammadhadi Bagheri, and Ronald M Summers. Chestx-ray8: Hospital-scale chest x-ray database and benchmarks on weakly-supervised classification and localization of common thorax diseases. In *Proceedings of the 2017 IEEE conference on Computer Vision and Pattern Recognition (CVPR)*, pages 2097–2106. IEEE, 2017.
- [121] Yifan Li, Yifan Du, Kun Zhou, Jinpeng Wang, Xin Zhao, and Ji-Rong Wen. Evaluating object hallucination in large vision-language models. In *Proceedings of the 2023 Conference on Empirical Methods in Natural Language Processing (EMNLP)*. ACL, 2023.
- [122] Haoning Wu, Zicheng Zhang, Erli Zhang, Chaofeng Chen, Liang Liao, Annan Wang, Chunyi Li, Wenxiu Sun, Qiong Yan, Guangtao Zhai, and Weisi Lin. Q-Bench: A benchmark for general-purpose foundation models on low-level vision. In *Proceedings of the 12th International Conference on Learning Representations (ICLR)*, 2024.
- [123] Christoph Schuhmann, Romain Beaumont, Richard Vencu, Cade W Gordon, Ross Wightman, Mehdi Cherti, Theo Coombes, Aarush Katta, Clayton Mullis, Mitchell Wortsman, Patrick Schramowski, Srivatsa R Kundurthy, Katherine Crowson, Ludwig Schmidt, Robert Kaczmarczyk, and Jenia Jitsev. LAION-5B: An open large-scale dataset for training next generation image-text models. In *Proceedings of the 36th Conference on Neural Information Processing Systems (NeurIPS)*, pages 25278–25294. Curran Associates Inc, 2022.
- [124] Christoph Schuhmann, Richard Vencu, Romain Beaumont, Robert Kaczmarczyk, Clayton Mullis, Aarush Katta, Theo Coombes, Jenia Jitsev, and Aran Komatsuzaki. LAION-400M: Open dataset of clip-filtered 400 million image-text pairs. *arXiv preprint arXiv:2111.02114*, 2021.
- [125] Minwoo Byeon, Beomhee Park, Haecheon Kim, Sungjun Lee, Woonhyuk Baek, and Saehoon Kim. COYO-700M: Image-text pair dataset [dataset]. <https://github.com/kakaobrain/coyo-dataset/>, 2022.
- [126] Piyush Sharma, Nan Ding, Sebastian Goodman, and Radu Soricut. Conceptual Captions: A cleaned, hypernymed, image alt-text dataset for automatic image captioning. In *Proceedings of the 56th Annual Meeting of the Association for Computational Linguistics (ACL)*, pages 2556–2565. ACL, 2018.
- [127] Soravit Changpinyo, Piyush Sharma, Nan Ding, and Radu Soricut. Conceptual 12M: Pushing web-scale image-text pre-training to recognize long-tail visual concepts. In *Proceedings of the 2021 IEEE/CVF Conference on Computer Vision and Pattern Recognition (CVPR)*, pages 3558–3568. IEEE, 2021.
- [128] Vicente Ordonez, Girish Kulkarni, and Tamara L Berg. Im2Text: Describing images using 1 million captioned photographs. In *Proceedings of the 24th International Conference on Neural Information Processing Systems (NeurIPS)*, page 1143–1151. Curran Associates Inc., 2011.
- [129] Ranjay Krishna, Yuke Zhu, Oliver Groth, Justin Johnson, Kenji Hata, Joshua Kravitz, Stephanie Chen, Yanis Kalantidis, Li-Jia Li, David A Shamma, et al. Visual Genome: Connecting language and vision using crowdsourced dense image annotations. *Int. J. Comput. Vis.*, 123:32–73, 2017.
- [130] Nisan Stiennon, Long Ouyang, Jeffrey Wu, Daniel Ziegler, Ryan Lowe, Chelsea Voss, Alec Radford, Dario Amodei, and Paul F Christiano. Learning to summarize with human feedback. In *Proceedings of the 34th Annual Conference on Neural Information Processing Systems (NeurIPS)*, volume 33, pages 3008–3021. Curran Associates, Inc., 2020.
- [131] Sander Schulhoff, Michael Ilie, Nishant Balepur, Konstantine Kahadze, Amanda Liu, Chenglei Si, Yinheng Li, Aayush Gupta, HyoJung Han, Sevien Schulhoff, et al. The prompt report: A systematic survey of prompting techniques. *arXiv preprint arXiv:2406.06608*, 2024.

- [132] Lin Chen, Jisong Li, Xiaoyi Dong, Pan Zhang, Conghui He, Jiaqi Wang, Feng Zhao, and Dahua Lin. ShareGPT4V: Improving large multi-modal models with better captions. In *Proceedings of the 2024 European Conference on Computer Vision (ECCV)*. Springer, 2024.
- [133] Dom Eccleston and Steven Tey. ShareGPT. <https://sharegpt.com/>, December 2023.
- [134] Wing Lian, Guan Wang, Bleys Goodson, Eugene Pentland, Austin Cook, Chanvichet Vong, and "Teknium". Slimorca: An open dataset of GPT-4 augmented FLAN reasoning traces, with verification [dataset], 2023.
- [135] Rohan Taori, Ishaan Gulrajani, Tianyi Zhang, Yann Dubois, Xuechen Li, Carlos Guestrin, Percy Liang, and Tatsunori B. Hashimoto. Stanford Alpaca: An instruction-following llama model. https://github.com/tatsu-lab/stanford_alpaca, 2023.
- [136] Canwen Xu, Daya Guo, Nan Duan, and Julian McAuley. Baize: An open-source chat model with parameter-efficient tuning on self-chat data. In *Proceedings of the 2023 Conference on Empirical Methods in Natural Language Processing (EMNLP)*, pages 6268–6278. ACL, 2023.
- [137] Baolin Peng, Chunyuan Li, Pengcheng He, Michel Galley, and Jianfeng Gao. Instruction tuning with gpt-4. *arXiv preprint arXiv:2304.03277*, 2023.
- [138] Abhishek Das, Satwik Kottur, Khushi Gupta, Avi Singh, Deshraj Yadav, José MF Moura, Devi Parikh, and Dhruv Batra. Visual dialog. In *Proceedings of the 2017 IEEE Conference on Computer Vision and Pattern Recognition (CVPR)*, pages 326–335. IEEE, 2017.
- [139] KunChang Li, Yinan He, Yi Wang, Yizhuo Li, Wenhai Wang, Ping Luo, Yali Wang, Limin Wang, and Yu Qiao. Videochat: Chat-centric video understanding. *arXiv preprint arXiv:2305.06355*, 2023.
- [140] Fuxiao Liu, Kevin Lin, Linjie Li, Jianfeng Wang, Yaser Yacoob, and Lijuan Wang. Mitigating hallucination in large multi-modal models via robust instruction tuning. In *Proceedings of the 20th International Conference on Learning Representations (ICLR)*, 2024.
- [141] Yanzhe Zhang, Ruiyi Zhang, Jiuxiang Gu, Yufan Zhou, Nedim Lipka, Diyi Yang, and Tong Sun. LLaVAR: Enhanced visual instruction tuning for text-rich image understanding. *arXiv preprint arXiv:2306.17107*, 2023.
- [142] Tao Gong, Chengqi Lyu, Shilong Zhang, Yudong Wang, Miao Zheng, Qian Zhao, Kuikun Liu, Wenwei Zhang, Ping Luo, and Kai Chen. Multimodal-GPT: A vision and language model for dialogue with humans. *arXiv preprint arXiv:2305.04790*, 2023.